Chaos, Solitons and Fractals 174 (2023) 113707

Contents lists available at ScienceDirect

Chaos, Solitons and Fractals

journal homepage: www.elsevier.com/locate/chaos

Long transients in discontinuous time-discrete models of population dynamics

Andrew Yu. Morozov [a,b,*], Dalal Almutairi [a,c], Sergei V. Petrovskii [a,d], Ying-Cheng Lai [e]

[a] School of Computing and Mathematical Sciences, University of Leicester, LE1 7RH, UK
[b] Laboratory of Behaviour of Lower Vertebrates, Institute of Ecology and Evolution, Moscow, 119071, Russia
[c] Department of Mathematics, College of Al-Muzahmiya, Shaqra University, Saudi Arabia
[d] Peoples Friendship University of Russia (RUDN University), 6 Miklukho-Maklaya St, Moscow 117198, Russia
[e] School of Electrical, Computer and Energy Engineering, Arizona State University, Tempe, AZ 85287, USA

ARTICLE INFO

Keywords:
Chaotic saddle
Chaotic repeller
Ghost attractor
Regime shift
Scaling laws
Intermittency

ABSTRACT

Traditionally, mathematical modelling of population dynamics was focused on long-term, asymptotic behaviour (systems attractors), whereas the effects of transient regimes were largely disregarded. However, recently there has been a growing appreciation of the role of transients both in empirical ecology and theoretical studies. Among the main challenges are identification of the mechanisms triggering transients in various dynamical systems and understanding of the corresponding scaling law of the transient's lifetime; the latter is of a vital practical importance for long-term ecological forecasting and regime shifts anticipation. In this study, we reveal and investigate various patterns of long transients occurring in two generic time-discrete population models which are mathematically described by discontinuous (piece-wise) maps. In particular, we consider a single-species population model and a predator–prey system, in each model we assume that the dispersal of species at the end of each season is density dependent. For both models, we demonstrate transients due to crawl-by dynamics, chaotic repellers, chaotic saddles, ghost attractors, and a rich variety of intermittent regimes. For each type of transient, we investigate the corresponding scaling law of the transient's lifetime. We explore the space of key model parameters, to find where particular types of long transients can be expected, and we show that long transients are omnipresent since they can be observed within a wide range of model parameters. We also reveal the possibility of complex patterns occurring as a cascade of transients of different types. We also considered a stochastic version of the model where some parameters exhibit random fluctuations. We show that stochasticity can reduce, extend or produce new patterns of long transients. We conclude that the discontinuity in population models significantly facilitates the emergence of long transients by creating new types and increasing parameter domains of the corresponding transient dynamics. Another important conclusion is that the asymptotic regime of population dynamics is hardly possible to predict based on a finite time course of species densities, which is crucial for ecosystem management and decision making.

1. Introduction

A large number of mathematical models in ecology are based on differential equations and/or discrete maps. In those models, the main focus has long been on the asymptotic states of the considered system, which are defined as the system attractors. The two main reasons are: (i) the relative simplicity of the asymptotic states as compared to the entire phase space (e.g., system equilibria can be found by solving algebraic equations), and (ii) the common sense belief that the time that it takes a real-world system to closely approach an attractor is not too long, therefore we can disregard the initial transient regime. There is, however, a growing understanding that the latter reason is essentially wrong, since a large number of theoretical models and empirical observations demonstrated that transient behaviour may persist over very long time periods [1,2]. In the case, where the length of transients is longer than the required horizon of our prediction, focusing solely on the long-term behaviour of systems would be misleading due to a mismatch of scales [3]. Correspondingly, there is a growing recognition of the leading role of transient dynamics, and especially long transients, in ecology and epidemiology, as well as applied dynamical systems of other origins [1,2,4–8]. Importantly, long transients are considered to be an alternative explanation of ecological regime shifts, where, unlike

* Corresponding author at: School of Computing and Mathematical Sciences, University of Leicester, LE1 7RH, UK.
E-mail address: am379@le.ac.uk (A.Y. Morozov).

https://doi.org/10.1016/j.chaos.2023.113707
Received 18 January 2023; Received in revised form 16 May 2023; Accepted 10 June 2023
Available online 12 July 2023

the classical tipping point scenario, a transients-related mechanism of shift occurs for constant model parameters [6,9].

Recently, the theoretical aspects of the long transients paradigm in ecological modelling have been revisited with the main goal of creating a more systematic approach based on the abundant literature on the topic [2,5,6]. To be able to predict regime shift due to the alternative transient-based scenario, the formal definition of a long transient has been proposed. The definition requires the existence of a scaling law for the transient lifetime when a certain bifurcation parameter tends to a critical value [5,10] (for detail see Section 2.2). Transient regimes have been classified according to their nature and their scaling [5]. On the other hand, despite hard efforts to systematise transient behaviour in models and empirical studies, this area of research still seems to be patchy and new types of transients are currently being revealed [8,11]. The current work is aimed to elucidate unknown features of transients in simple time-discrete population models.

Population dynamics models based on maps (i.e., assuming non-overlapping generations) have been in the focus of theoretical ecology for more than half a century starting from the seminal works of R. May [12–15]. Various patterns of long transient have been reported in discrete time models. For example, the possibility of chaotic saddles was demonstrated for generic model settings, where the trajectory seems to be chaotic for a long time before it becomes eventually periodical [16]. Importantly, chaotic saddles and super-persistent chaotic saddles were shown to exist within a wide range of a model parameter, which is crucial from the practical point of view to observe chaos, which is a fundamental problem in ecology [17,18]. Indeed, from the general theory of discrete maps it follows that in the parameter space windows corresponding to periodic orbits are dense [19,20], whereas parameter sets for chaotic attractors are extremely scarce, they contains no open intervals and constitute a fat fractal set [21,22]. In contrast, for transient chaos, there are an infinite number of open parameter intervals, which can be observed in experiments/observations which is not possible for a 'pure' chaotic behaviour [13]. Emergence of transient chaos requires some restrictions on the model: the minimum dimension is two for invertible discrete maps [23,24].

We should stress, however, that despite a large body of literature, our understanding of long transients in discrete population models is still limited even regarding relatively simple single-species and two-species models [16]. There are at least two major gaps in our knowledge. Firstly, the transient phenomena are much less understood in maps including discontinuity despite the fact that such models are widely used in ecology and ecosystem management. For example, piece-wise discrete models are used in the theory of optimal harvesting, species conservation, and pest control [25–28]. The existence of long transients can significantly alter the control strategy proposed in those models under asymptotic dynamics settings. On the other hand, it is known that discrete models with discontinuous functions can possess complicated dynamics and a complex bifurcation structure quite different from those observed in the corresponding models without discontinuity; for example in such systems, the classical period-doubling bifurcation scenario may not necessarily hold [29]. Therefore, it is important to understand what mechanisms of long transients can occur in such systems [30]. The second gap in our knowledge is the substantial lack of understanding of the structure of the parameter space corresponding to various types of transients. For example, a crucial question is whether parameter values corresponding to long transients make up a substantial proportion of the overall parameter space. Apparently, this issue has important practical applications. Another interesting aspect requiring more attention is the possibility of the switch different types of transients before approaching the final attractor, i.e. the existence of a cascade of transients [31]. One efficient technical way to reveal the commonality of long transients is through the construction of the corresponding parametric diagrams; however, to the best of our knowledge, this approach is not well-developed in the literature even for simple models despite some recent progress [32–34]. Finally, the role of the initial condition in the transient behaviour has not been properly studied; in particular, a largely open question is how sensitive the long transients are to the choice of the initial conditions.

In this paper, we endeavour to address the above-mentioned gaps, although our research into the problem is by no means exhaustive. Namely, we explore transient behaviour in two discrete models of population dynamics containing discontinuity in model functions. The models are: a single species population model and a predator–prey model, in each model we include the effects of density dependent migration described by a discontinuous term. In each model, we reveal patterns of long transient dynamics due to various mechanisms and we explore their scaling behaviour. We discover some new types of transients which emerge due to the discontinuity in the model. We construct bifurcation diagrams to reveal the structure of parameter space corresponding to different transient regimes and demonstrate that transients are omnipresent in the considered systems. Interestingly, some patterns show cascades of transients, when dynamics switch between different transient types before finally, the trajectory settles on an attractor. We demonstrate that the sets of parameters producing long transients have a complex structure. We also discuss the dependence of transients on the initial condition. Along with purely deterministic models, we explore effects of random fluctuations of model parameter on long transients. Finally, we link our findings to the challenges of ecosystem management.

2. Theoretical framework

2.1. Model equations

Here we assume non-overlapping generations (e.g. such an assumption is usually made in modelling insect populations [15]), and consider two simple discrete population models with density dependent dispersal. Firstly, we consider a single species model. The generic form of the model is given by [26]

$$\tilde{X}_{t+1} = F(X_t), \tag{1}$$

$$X_{t+1} = \tilde{X}_{t+1}(1 + \epsilon_1 sgn(X_t - \tilde{X}_{t+1})), \tag{2}$$

where $\tilde{X}_{t+1}$ is the population size at the end of year t prior to the dispersal; X_t is the population size at the end of year t after the dispersal event. The function F denotes the local population growth. The biological rationale behind the model is the following. Each year the population locally grows according to the function F, then before the end of the season, a part of the population undergoes dispersal from the given geographic location to some other sites. The dispersal is density dependent. In the case where the density at the end of the growth season is higher as compared to the last year population density, i.e. $X_t < \tilde{X}_{t+1}$, a part of the population leaves the given site. In the opposite situation, i.e. when $X_t > \tilde{X}_{t+1}$, individuals from other sites arrive at the given location, thus we have an inflow of population. The parameter ϵ_1 characterises the strength of dispersal. Another interpretation of the term $\epsilon_1 sgn(X_t - \tilde{X}_{t+1})$ can be the effect of ecosystem management, where some proportion of individuals is removed or added depending on the previous year's density and the density after the growth season.

The above model containing two equations can be re-written as a single equation discrete map

$$X_{t+1} = max\left[F(X_t)(1 + \epsilon_1 sgn(X_t - F(X_t))), 0\right] \equiv H(X_t). \tag{3}$$

Taking the maximum in the above expression excludes unrealistic cases where either X_t or $F(X_t)$ becomes negative. The resultant map is given by the function $H(X_t)$, which is a discontinuous function.

The second model is a discrete predator–prey system which is an extension of the above single species model, where a dynamical predator is added. The local population growth is described by the Lotka–Volterra discrete equations (see [35,36]). Unlike the previous

studies, we introduce the density dependent discontinuous dispersal terms in the same way as in the single species model. The corresponding equations are given by

$$\tilde{X}_{t+1} = G_1(X_t, Y_t) \equiv F(X_t) - bX_tY_t, \tag{4}$$

$$\tilde{Y}_{t+1} = G_2(X_t, Y_t) \equiv dX_tY_t - cY(t), \tag{5}$$

$$X_{t+1} = max\left[\tilde{X}_{t+1}(1 + \epsilon_1 sgn(X_t - \tilde{X}_{t+1})), 0\right], \tag{6}$$

$$Y_{t+1} = max\left[\tilde{Y}_{t+1}(1 + \epsilon_2 sgn(Y_t - \tilde{Y}_{t+1})), 0\right], \tag{7}$$

where X_t, Y_t is the population sizes of the prey and the predator, respectively, at the end of year t after the dispersal event; $\tilde{X}_t, \tilde{Y}_t$ are the population sizes prior to the dispersal. $F(X)$ is the growth rate of the prey in the absence of the predator. The parameter $c > 0$ describes the mortality of the predator in the absence of prey; $b > 0$ is the attack rate of the predator on the prey, and $d > 0$ is the combination of the attack rate and the trophic efficiency of the predator. Without losing generality we can assume that $b = 1$ (e.g. by re-scaling the density of predator). The dispersal terms have the same meaning as for the single species model. The four-dimensional system above can be easily simplified to a two-dimensional system as follows

$$X_{t+1} = max\left[G_1(X_t, Y_t)(1 + \epsilon_1 sgn(X_t - G_1(X_t, Y_t))), 0\right], \tag{8}$$

$$Y_{t+1} = max\left[G_2(X_t, Y_t)(1 + \epsilon_2 sgn(Y_t - G_2(X_t, Y_t))), 0\right], \tag{9}$$

where the functions $G_1(X_t, Y_t)$ and $G_2(X_t, Y_t)$ are defined above. For simplicity, to reduce the number of parameters, in the rest of the text we will assume that $\epsilon_{1,2} \equiv \epsilon$.

One needs to parameterise the growth rate function $F(X)$ in both models. Following the work of [26], here we mostly focus on the case where $F(X)$ is the logistic function, i.e. $F(X) = \mu X(1 - X)$, where μ is the maximal per capita growth rate of the population X. However, in order to check the robustness of our findings to the choice of the growth function, we have also briefly considered the scenario where $F(X)$ was given by the Ricker function given by $F(X) = X \exp(\mu(1 - X))$. For the Ricker function we find similar mechanisms generating long transients which we do not present here for the sake of brevity. Note that the fixed points of model (3) with $\epsilon_1 > 0$ were studied in [26], whereas system (8) without dispersal terms ($\epsilon_{1,2} = \epsilon = 0$) was briefly considered in [35,36]. Here, however, our main focus will be on transient dynamics. For each transient type, we explore the scaling properties of transients, which is their fundamental property [5] (see also the definition of transients in the next subsection).

Finally, along with the deterministic models presented above, we also considered stochastic versions of the same models, where some coefficients exhibit random fluctuations. The details on the stochastic versions of the models are provided in Section 3.3.

2.2. Defining a long transient

To reveal long transient regimes in the above models, we need some formal definition at hand. We should stress, however, that transient phenomena in dynamical systems (either for time continuous or discrete dynamical systems) are much more diverse to be covered by an exhaustive single definition. As a result, various definitions of transients currently exist in the theoretical literature which can be applied to modelling different phenomena [5,8]. Moreover, a universal, all-embracing definition would be potentially meaningless. Indeed, strictly speaking, trajectories which are not a part of the system's attractor should be formally considered as transients. On the other hand, we argue (see below) that even if the considered trajectory is exactly an attractor (or it is close to an attractor), sometimes parts of this trajectory can be sensibly considered as long transients. In this study, we shall use the definition from the recent study by Morozov et al. [5], which relates a long transient to a regime shift.

Definition 2.1 (*Long Transient Dynamics*)**.** Consider a dynamical system (discrete or continuous), where all parameters are constant, i.e. they do not depend on time. We assume that the system is functioning in a particular state (a 'quasi-stable regime'), where the main characteristics remain close to constant. Note that we understand a 'quasi-stable regime' in a broad sense, including oscillatory dynamics as well. Suppose that at some point the system experiences a transition to another regime which is stable (or quasi-stable) and the transition occurs on a timescale much shorter than the duration of the preceding dynamical pattern. If the duration of the system state before the transition can be made as long as possible, when approaching some bifurcation parameter, we call it a long transient. Note that the new regime after the shift can be a long transient as well. The above definition can be applied for a stochastic system as well in the case random fluctuations of a model parameter are small and they occur around some mean value.

Remark. Note that in this paper, unlike in the study by Morozov et al. [5], we intentionally do not consider another important class of transients, where the system's dynamics evolve on a very slow timescale, which is much longer than any characteristic time of the current dynamical pattern before reaching a different stable or to a different quasi-stable regime (e.g. damped oscillations with very slow changing amplitude, which can be found in both considered models). Such long transients should be explored elsewhere. Also, here we do not make a distinction between chaotic and non-chaotic transients, despite the fact that the former may have different properties.

Remark. The proposed definition assumes the existence of scaling behaviour of the average lifetime of a long transient. In other words, if some control parameter p tends to a critical value p_c, the average lifetime will tend to infinity according to some law which is usually exponential, power law or their combination. Various scaling behaviour allows for the classification of distinct transient patterns [5,10].

Remark. We should stress that according to the above definition, long transient dynamics can be a part of an intermittent regime, when the system remains on the attractor or stays close to an attractor, which is characterised by different phases of dynamics. For example, a long (transient) phase of low amplitude oscillations can be followed by large amplitude oscillations. By varying a model parameter we can make the duration of one as large as possible, i.e. the lifetime of the phase exhibits scaling. From the ecological point of view, the inclusion of intermittency-related transients (where the trajectory is a final attractor) is required in the case we model phenomena involving various time scales [5,37].

Note that although we require a long transient to have a lifetime which can be made as large as possible, in this paper, the diagrams showing the presence of long transients are constructed by fixing some minimal lifetime of transients T. In the context of any particular ecological application, the choice of T can be linked to species traits and/or to a typical timescale of ecological management actions. Finally, although some transient regimes can be found using analytical techniques, most transients patterns (especially for the predator–prey model) were obtained via numerical simulations (we used MATLAB software [38]).

3. Results

3.1. Transients in the single species model

We implemented extensive numerical simulations as well as some analytical methods to reveal long transients in model (3). The main types of long transients are briefly summarised in Table 1. Note the table provides a joint classification of transients for both models. The corresponding numerical examples of each type of transients in model

Table 1
Classification of long transients in model (3) and model (8). Symbols '*' and '**', refer, respectively, to the one-dimensional and the two-dimension case; p is a control parameter; p_c is its bifurcation value, we assume $|p-p_c| \ll 1$. The transient lifetime τ is understood as follows: for recurrent transients, τ is estimated via averaging over a long time period; for non-recurrent transients, τ is obtained by averaging over a set of initial conditions; for non-recurrent and non-chaotic transients, τ is computed based on a fixed initial condition. Details on calculating scaling of transients are provided in the text.

Transient type	Scaling behaviour	Numerical examples
Transients generated by a ghost attractor (smooth scenario)	$\tau \propto \frac{1}{\lvert p-p_c\rvert^{0.5}}$	Fig. 1A*, Figs. 5A**,B**
Transients generated by a ghost attractor (discontinuous scenario)	$\tau \propto -\log\lvert p-p_c\rvert$	Fig. 1B*, Figs. 5C**,D**
Transients generated by chaotic repellers or chaotic saddles	$\tau \propto \frac{1}{\lvert p-p_c\rvert^{\gamma}}$, $\gamma \geq 1$	Figs. 1C*,D* Figs. 6A**,B**,C**,E**
slow-fast dynamics (smooth/discontinuous scenarios)	$\tau \propto \frac{1}{\lvert p-p_c\rvert^{\gamma}}$, $\gamma \geq 1$	Figs. 1E*,F*, Figs. 6D**,F**
Transients due to non-chaotic saddles	$\tau \propto -\log\lvert p-p_c\rvert$	Figs. 5E**,F**

(3) are shown in Fig. 1. We have also estimated the scaling behaviour of the lifetime of transients, which in most of cases is obtained via averaging over the time or initial conditions (more detail on computation of the lifetime of each type of transients is provided below).

We find that the simplest generic class of long transients in the model is due to the so-called ghost attractor with the corresponding examples shown in Figs. 1A,B. The general aspects of ghost attractors are described in [5,39,40]. The given type of transient occurs when a stable periodic orbit with period n disappears when some control parameter p has been varied (here p is ϵ or μ). Assume that we initially have a stable periodic orbit with the period n, i.e. $H^n(X) = X$. Disappearance of the periodic orbit occurs at some critical value of bifurcation parameter p_c, and a small gap (called the escape channel) is formed between the model function $H^n(X)$ and the line $X = X$. The time that the trajectory spends when travelling through the escaping channel shows a scaling behaviour as a function of the difference $|p-p_c|$. In our model, emergence of a ghost attractor occurs in two different ways. According to the smooth scenario, the loss of stability occurs when a pair of stable/unstable periodic orbits annihilates at $p = p_c$. It can be shown that the lifetime of a transient is scaled as a power law, $\tau \propto \frac{A_1}{(p-p_c)^{0.5}}$, where A_1 is a positive constant [5,41]. An example of a transient according to the considered scenario is given in Fig. 1 A for a two-periodic orbit (the schematic flowchart of the emergence of a ghost attractor is provided in SM1, some transients due to ghost attractors with a higher periodicity are shown in SM2).

A different scenario of transients generated by a ghost attractor is possible when the disappearance of the stable periodic orbit takes place at a point of discontinuity of the system. An example of the corresponding transient pattern is shown in Fig. 1B. The scaling behaviour is given by $\tau \propto -A_2 \log|p-p_c|$, where A_2 is a positive constant. This law can be understood using the flowchart from Fig. 2, the upper panel, the point of discontinuity is shown by a dashed vertical line. Before the bifurcation, the system has a periodic orbit defined by $H^n(X) = X$, which is locally stable (shown by a filled circle). After the bifurcation, $H^n(X)$ and X do not intersect in the considered vicinity. Near the point of discontinuity, the function $H^n(X)$ can be approximated by a straight line with a slope K $(1 > K > 0)$. The distance η between $H^n(X)$ and $X = X$ at the point of discontinuity is approximately proportional to $|p-p_c|$, i.e. $\eta \propto |p-p_c| \ll 1$. The trajectory approaches the point of discontinuity from some distance apart (we can consider this distance to be of order 1). It will require τ steps for the trajectory to reach the point of discontinuity, which can be found from $\eta = K^{\tau}$. We have $\tau \propto \log|p-p_c|/\log(K) = -A_2 \log|p-p_c|$, $A_2 > 0$ since $\log(K) < 0$. Note that for the discontinuous scenario of the ghost attractor, the transient lifetime increases at a much slower rate as compared to the smooth scenario. We should also stress that in both mentioned cases, the trajectory can eventually return to the vicinity of the ghost, thus the transient will be a part of a larger attractor (chaotic or periodic). Note that for both above mentioned types of ghost attractors, we measure the lifetime based on the closeness to the ghost (e.g. requiring that the trajectory should not deviate from the ghost of the fixed point more than 5%–10% of its value).

Another scenario of long transients involves chaotic repellers. A typical example of a chaotic transient is shown in Fig. 1C, where the system exhibits apparently chaotic dynamics with large amplitude oscillations before the trajectory becomes trapped within some narrow region. The asymptotic regime can be a vicinity of the point of discontinuity of the function $H(X)$, which is $X = (\mu-1)/\mu$, or this can be some periodic orbit. The scaling law of chaotic transient lifetime is $\tau \propto \frac{A_3}{(p-p_c)^{\gamma}}$, which is in agreement with previous studies [5,41]. We should note, however, that we obtained the scaling law only for $\epsilon \to 0$, thus here $p = \epsilon$. Transient chaos can also include patterns of intermittency, where large amplitude and low amplitude phases alternate before the trajectory can find an escaping channel. An example of a transient due to chaotic repeller with transient intermittency is shown in Fig. 1D. The end of this type of transients can be determined when the trajectory approaches some vicinity of the new attractor (e.g. to be within 5% error band).

Chaotic intermittency with fast and slow oscillations can be the eventual attractor of model (3). However, different phases of intermittency can be made as long as possible by tuning a model parameter. Therefore, we can still apply the definition of the long transients to a particular phase. For example, small amplitude oscillations can last for a long time before the system starts the next phase with large amplitude oscillations. An example of long transients due to intermittency is shown in Fig. 1E, where the dynamical regime characterised by small amplitude oscillations can last for a long time. The mechanism of transients consists in trapping the trajectory within a small region before the trajectory finds some route to escape from the trap (a trapping region can occur for some period $n > 1$, in this case, the resultant pattern will be close to an n-periodic solution). We find that the emergence of a small trapping region can include two different mechanisms. Firstly, this can be related to the discontinuity of the function $H(X)$. The corresponding flowchart is shown in Fig. 2 (the middle row). In Fig. 2C, once the trajectory lands inside, it would stay within the trapping region forever. However, for a slight variation of the model parameter p, a small escaping channel emerges in the trap: the trajectory will leave the trap within some finite time (Fig. 2D). To do this, it should land within a small band (escape channel) whose length is proportional to the difference $|p-p_c|$, thus the scaling of the transient lifetime is given by $\tau \propto \frac{A_4}{|p-p_c|}$. The critical value p_c, indicating the emergence of an escaping channel is derived in Appendix A.

The second class of a trapping region related to intermittency occurs for periodic trajectories generated by $H^n(X)$, within an interval of X which does not contain a discontinuity. The corresponding numerical

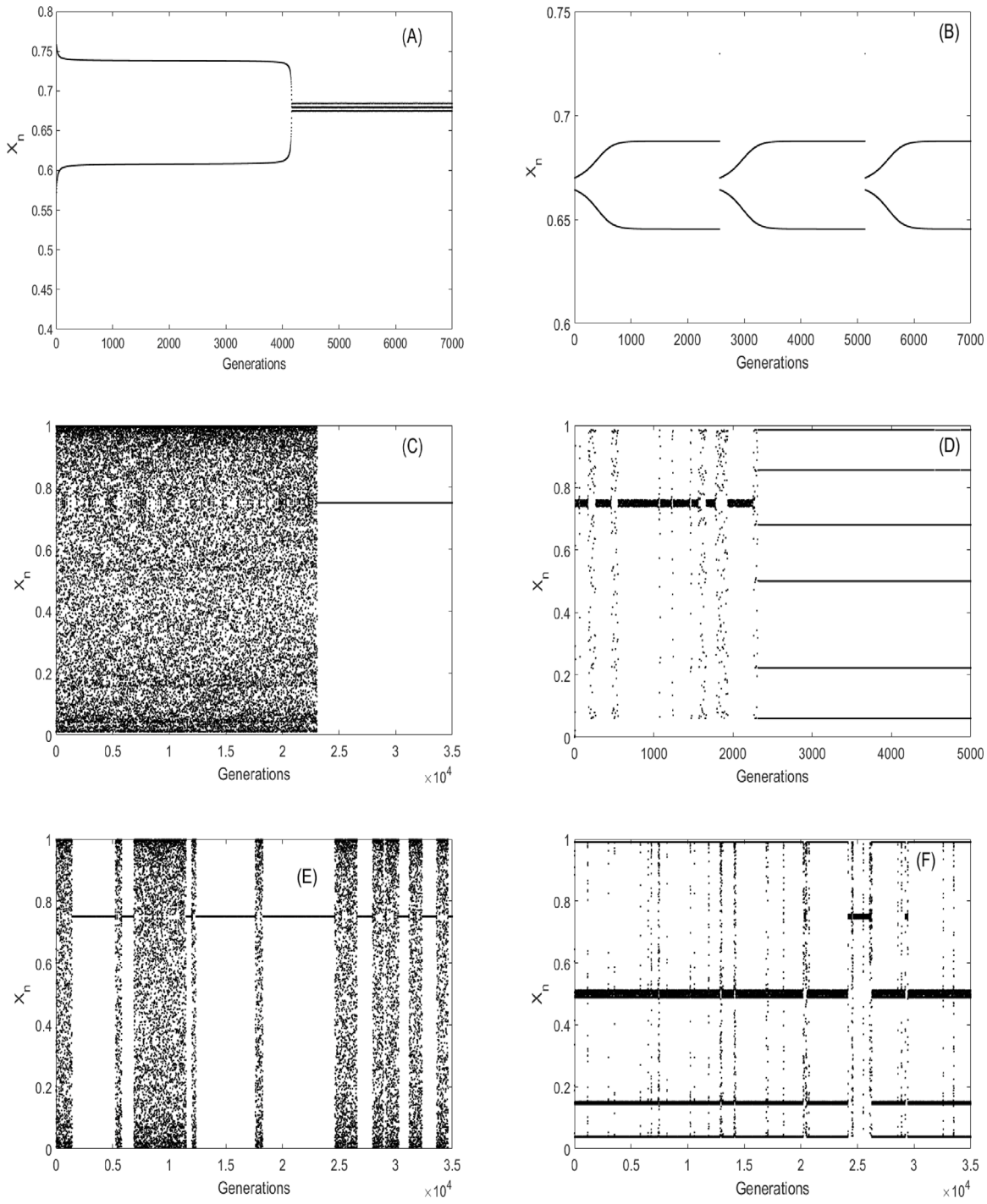

Fig. 1. Main types of long transients in the single species model (3), $F(X) = \mu X(1 - X)$. (A) Transient generated by a ghost attractor of a stable periodic orbit (smooth scenario), $\mu = 3.12$, $\epsilon = 0.007647$, $X_0 = 0.00098322$. (B) Transient generated by a ghost attractor of a stable periodic orbit (discontinuous scenario), $\mu = 3.2$ $\epsilon = 0.061251098$; $X_0 = 0.67$. (C) Transient generated by a chaotic repeller, $\mu = 4$, $\epsilon = 0.015$, $X_0 = 0.0000873$. (D) Transient generated by a chaotic repeller with transient intermittency, $\mu = 3.99$, $\epsilon = 0.00013$, $X_0 = 0.009475$. (E) Asymptotic intermittency involving a discontinuous trapping region, $\mu = 4$, $\epsilon = 0.00109$, $X_0 = 0.05$. (F) Asymptotic intermittency involving continuous and discontinuous trapping regions, $\mu = 4.00032654$, $\epsilon = 0.0095$, $X_0 = 0.05$. Details on the mechanisms of transients are provided in the text.

example is shown in Fig. 1F. In fact, Fig. 1F shows a combination of two patterns of intermittency: one is the intermittency due to the trajectory being trapped around the point of discontinuity, and the second one includes a phase close to a periodic orbit (with $n = 4$), where the trapping region is smooth. Fig. 3 (the bottom row) shows the mechanism of trapping trajectory within a small region which does not contain discontinuity. Overall, the mechanism triggering a transient is conceptually similar to that of the discontinuous scenario, therefore the scaling law of the lifetime is the same. However, the critical value of control parameter p_c resulting in opening an escape channel can be found from a different condition $H^n(X^{**}) \approx \hat{X} = H^n(\hat{X})$, where X^{**} is the local minimum of $H^n(X)$, and $\hat{X}$ is the closest unstable n-periodic orbit located on the right of X^{**}. For both cases of intermittency, the scaling laws for the small amplitude phase are provided in SM3. On the other hand, the large amplitude phase (fast dynamics) presents a transient regime as well, which is due to a chaotic repeller (the chaoticity was verified via following exponential deviation of close trajectories). However, in this case, it is hard to derive the

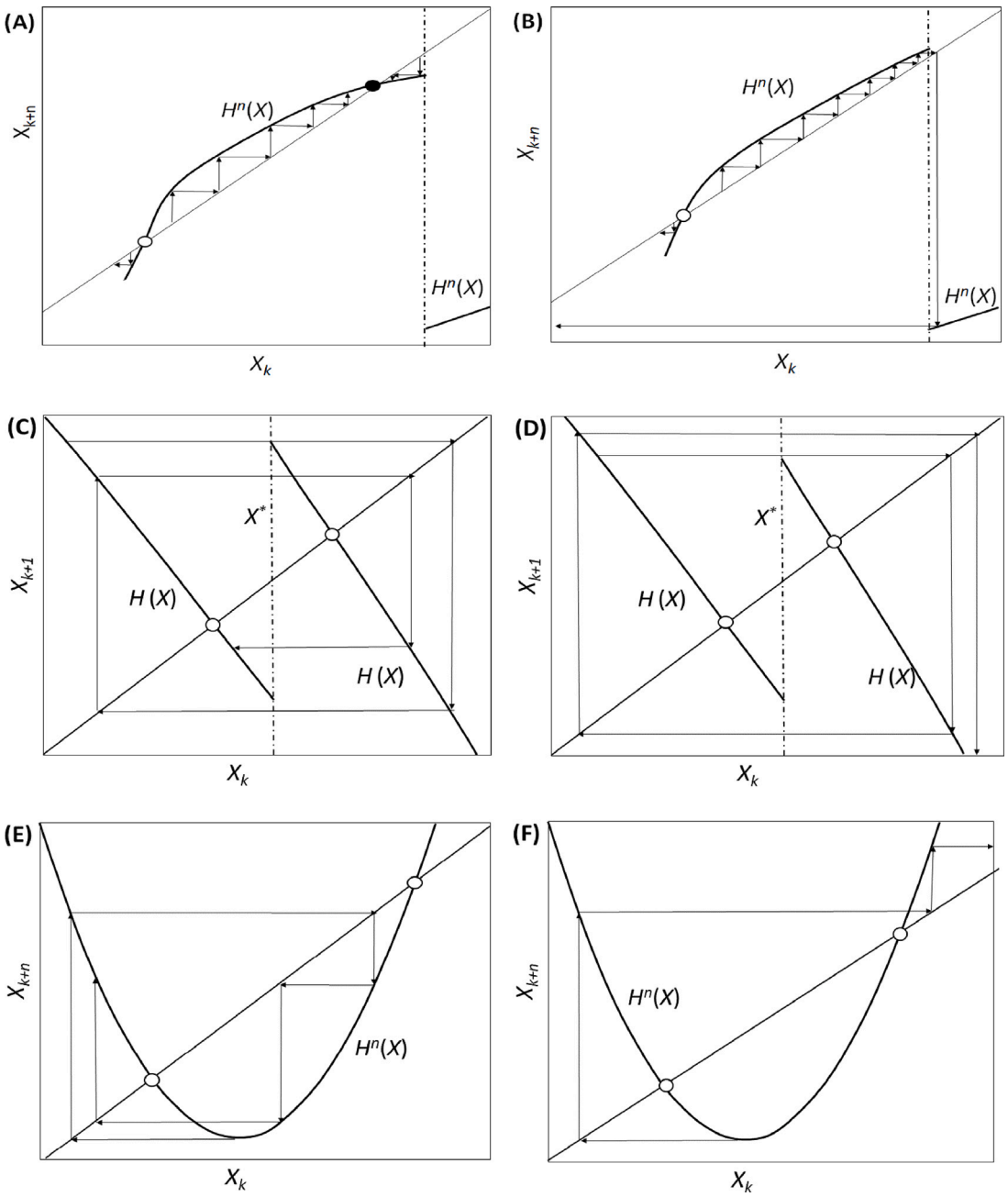

Fig. 2. Mechanisms of the emergence of long transients in the single species model (3), $F(X) = \mu X(1 - X)$. Upper panel: transients generated by a ghost attractor emerging via a discontinuous scenario (for the continuous scenario, see SM1). (A) Locally stable periodic orbit (filled circle). (B) The stable orbit disappears at the point of discontinuity; this creates a small escaping channel for the trajectory. The trajectory stays for a long time near the point of discontinuity before it goes away. Middle panel: transients due to slow-fast intermittency via a discontinuous scenario. (C) The trajectory is trapped within a region located around the point of discontinuity X^*. (D) Variation of a model parameter creates a small escaping channel, so after spending a long time (characterised by slow changes), the trajectory eventually leaves the trap to start fast phase of dynamics. Lower panel: transients due to slow-fast intermittency via a smooth scenario. (E) The trajectory is trapped within a small region located around the local minimum of $H^n(X)$. (F) Variation of a model parameter creates a small escaping channel, so after spending long time, the trajectory eventually leaves the trap to start a fast phase (large amplitude) of intermittency. Open circles represent unstable fixed points.

corresponding scaling law analytically. We numerically found that the chaotic phase of intermittency regime becomes infinitely large only when $\epsilon \to 0$.

For all types of intermittency-related transients, we investigated the law of distribution of the transient lifetime. We generally found the distribution to follow the exponential law at the tail both for the small amplitude and the large amplitude phase (see SM3 for detail). Therefore, the transient lifetime should be understood as the mean value of the mentioned distribution. The length of a small amplitude phase of the transient can be defined as the moment of time, when the trajectory leaves the trap shown in Fig. 2.

We investigated the dependence of occurrence of various types of transients in (3) on the model parameters, μ and ϵ. In our studies, we mainly focused on the small values of parameter ϵ (approximately up to $\epsilon = 0.1$), and we mostly varied μ from $\mu = 3$ until its maximal possible values assuring the positivity of X_k. The typical diagrams are presented in Fig. 3. The diagrams were constructed via direct computer simulation by following the system's dynamics within $T = 10{,}000$ generations. For each parameter set, 200 first generations are disregarded. We should stress, however, that the system is rather sensitive to variation of model parameters even by a very small value which can be seen by zooming some parts of diagrams (see Fig. 3C,E). For example, variation of the

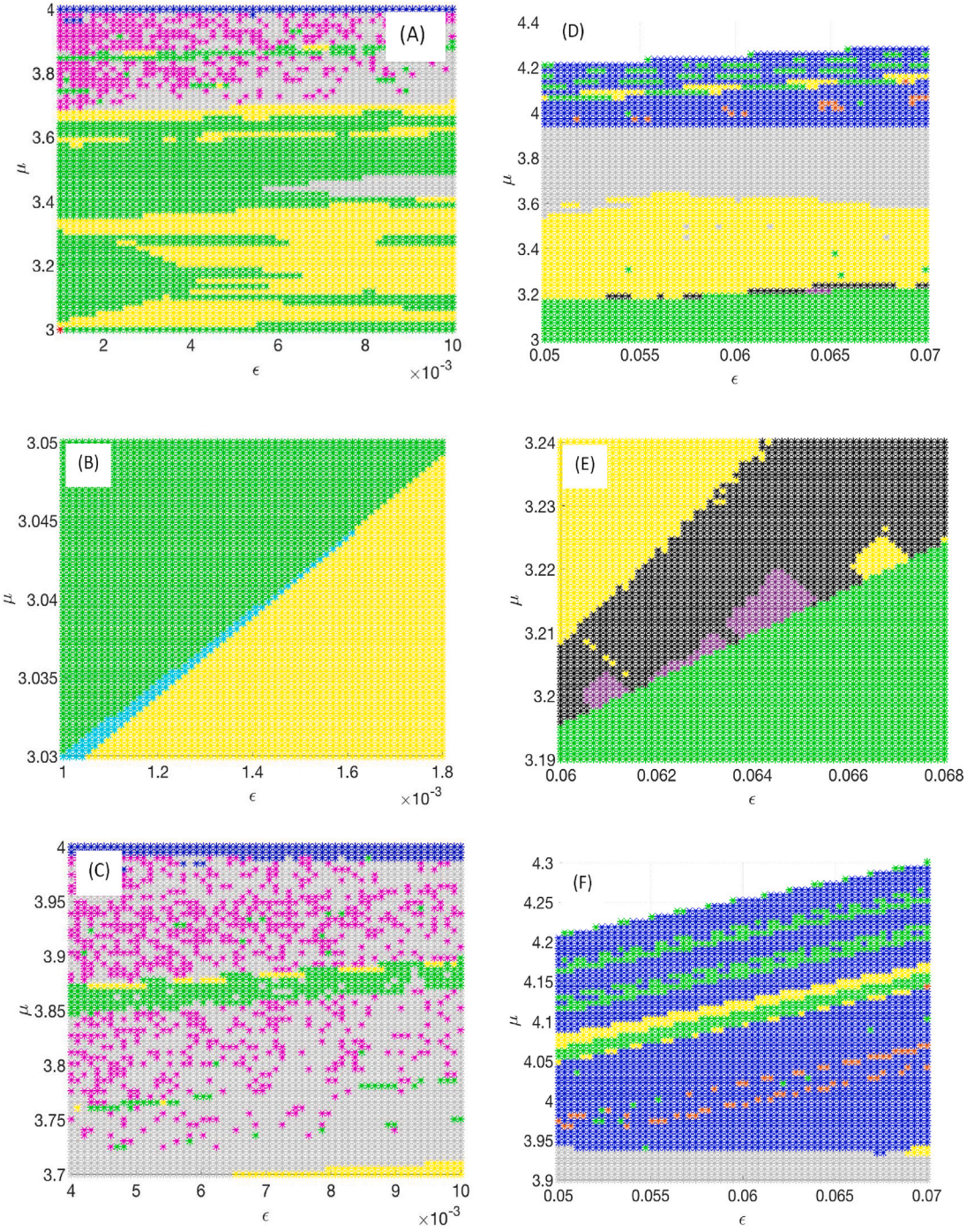

Fig. 3. Dependence of transients on parameters ϵ and μ in the single species model (3), with the logistic function, the starting point is $X_0 = 0.7$. The upper panel shows the main diagrams constructed for small and intermediate values of ϵ; the middle and the bottom panels provide fine resolutions of the diagrams in the upper panel. The observed long transient patterns include: ever persistent intermittency with fast and slow phases (dark blue); transients due to chaotic repellers (magenta); transients due to chaotic repellers with intermittency (orange); transients generated by a ghost attractor via continuous scenario (cyan); transients generated by a ghost attractor via discontinuous scenario (dark red). Black colour indicates trajectories recurrently spending large time near an unstable fixed point. Other colours denote realisations of trajectories without long transients; in this case, the final attractors include: stable periodic orbits (green); chaotic behaviour without intermittency (yellow); chaotic dynamics, where the trajectory is quickly trapped and always stays near the point of discontinuity (defined as $|X_t - X^*| < \epsilon$, grey colour). White colour corresponds to extinction of the species. (For interpretation of the references to colour in this figure legend, the reader is referred to the web version of this article.)

parameter ϵ by 10^{-5} in some domains can entirely change the pattern of dynamics and cause creation or suppression of a transient. Therefore, the figures only provide a coarse representation of the underlying diagrams. Along with long transient patterns, a large portion of points in the diagram indicates non-transient scenarios, where the trajectory quickly approaches either chaotic (but not intermittency-based) or periodic attractors.

Overall, we find that long transients are mostly observed when μ varies from 3.7 up to the maximal possible value of this parameter for the given ϵ. For small values of ϵ (see Fig. 3A), the most frequently observed transients (in terms of numbers of the parameter sets for which they were revealed) are those due to chaotic repellers depicted by magenta stars. The transients due to permanent slow-fast intermittency are observed near for μ close to $\mu = 4$ (dark blue stars). The

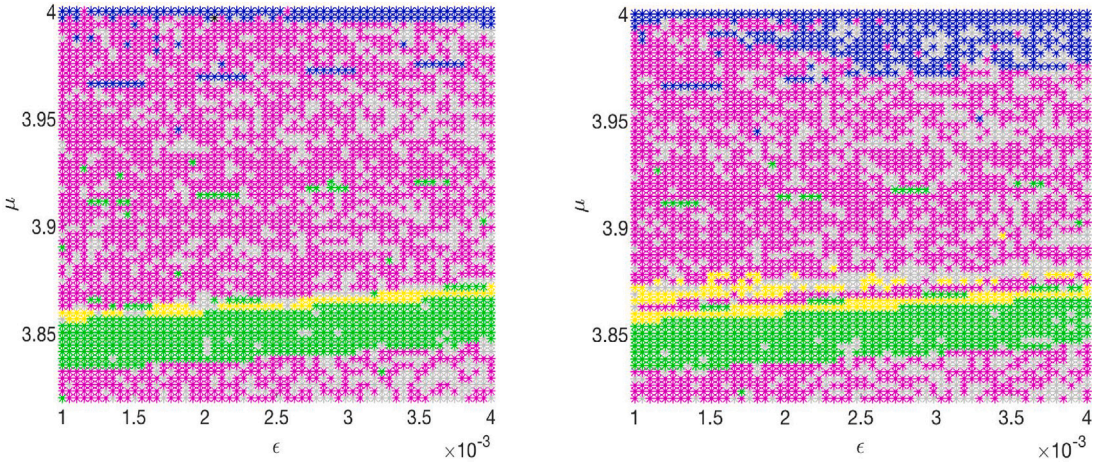

Fig. 4. Dependence of long transients in model (3) with the logistic function on initial conditions used. Both diagrams in the right column are constructed starting from $X_0 = 0.7$, whereas the diagrams in the left column are obtained for $X_0 = 0.5$. The time of simulation is $T = 10{,}000$ generations, 200 first generations are disregarded. The meaning of the colours for the domains is the same as in Fig. 3. (For interpretation of the references to colour in this figure legend, the reader is referred to the web version of this article.)

domains corresponding to ghost attractors (cyan stars) are smaller in size, as compared to other types of transients. An example of a domain containing a ghost attractor via a smooth scenario is shown in Fig. 3B. For larger values of ϵ (see Fig. 3D), the most frequently observed transients become those related to permanent (asymptotic) slow-fast intermittency. Another interesting transient pattern includes transient intermittency (orange stars in the diagram), where the trajectory after exhibiting several fast and slow phases become periodic (see Fig. 1D for an example of transient dynamics). Transients generated by a ghost attractor via discontinuous scenarios are observed for some intermediate values of μ, this is presented in Fig. 3E (dark red). Note that there are also dynamical regimes, where the trajectory is recurrently sent to a vicinity of an unstable equilibrium, where it can stay for a long time (an example is provided in SM2, panel A). In the diagram, such patterns are shown in black.

Although the boundary for the asymptotic slow-fast intermittency is given by a smooth curve (see Appendix A for analytical derivation), the parameter sets corresponding to this regime in the diagram are rather patchy. This can be seen from Figs. 3C,F, which provide finer resolutions of the parametric diagrams around $\mu = 4$. One can see that the dark blue domain of intermittency contains a large number of small inclusions, corresponding to either non-transient dynamics or transients of a different type. This is explained by the possibility of simultaneous presence of other attractors and by the fact that a long transient might requires particular initial condition (otherwise the trajectory quickly approaches an attractor without producing a long transient).

Finally, we briefly considered the dependence of long transients on the initial condition, a typical outcome is shown in Fig. 4. As previously, we focus on the values of μ close to 4. The diagrams are constructed for two different initial conditions: $X_0 = 0.7$ and $X_0 = 0.5$. Although the generic structure of the diagrams is preserved, one can see important difference between the right and the left columns. A comprehensive comparison of diagrams reveals a few major factors which make them different. Namely, the chaotic nature of transients may result in a large variation of the transient lifetime: the time of finding an escaping channel can be either increased or be reduced. In particular, the trajectory can be trapped by the transient regime for a period of time larger than the time of observation T, in this case, we will classify such regime as asymptotic. The existence of alternative attractors can largely affect the presence of transients.

3.2. Transients in the predator–prey model

In this section, we discuss long transients found in the predator–prey model (8). We should say, however, that due to the extreme complexity of the system caused by an extra dimensionality and also due to the presence of a discontinuity in both equations, it becomes technically impossible to exhaustively span the entire parameter space to be able to uncover all types of transients. We limit our study to fixing some parameters and varying the others. When revealing the scaling law of transients, we consider the control parameter p to be either ϵ or μ, as in the single species model. However, we found that variation of other parameters (e.g. d or c) would generally result in the same scaling laws (except cases where creation of transients requires approaching of a parameter to zero). Overall, in our search for long transients, we have completed approximately 10^5 numerical simulations. The main types of long transients in model (8) are presented in Figs. 5, 6. Table 1 contains basic information on the types of transients in the system, their scaling properties as well as illustrative examples. Scaling laws of transients in (8) ares provided in SM5.

Fig. 5 presents main types of long transients which can be characterised as non-chaotic: they include ghost attractors-mechanisms and non-chaotic saddles. Fig. 5A gives an example of a transient due to ghost attractor, which is realised via a smooth scenario. According to this scenario, a saddle point and a stable node collide as a result of a saddle–node bifurcation, and the trajectory becomes trapped in the vicinity of the previously existing fixed points (see SM1 for a schematic presentation of the mechanism). The existence of a pair of closely located saddle and stable node fixed points was validated by generating a large number of trajectories from different initial conditions (we do not provide the corresponding figures for brevity). We find that the scaling of the transient lifetime is the same as in model (3). Note that shown in the example of Fig. 5A, the periodicity of fixed points (before the bifurcation) is $n = 6$, this generates a long transient with the same periodicity. Note that the transient behaviour becomes recurrent: the trajectory returns to the vicinity of the saddle–node ghost and spends there a large portion of time. The transient dynamics is a large part of the overall attractor which exhibits a cyclic-like behaviour, which is, however, not exactly periodical. Fig. 5B presents the prey and predator densities plotted every $n = 6$ generations. One can see from this graph that the trajectory mostly stays near some fixed point and quickly jumps to the vicinity of another. The scaling of this transient follows a power law (see SM5 for details).

Fig. 5B,C give an example of a transient due to a ghost attractor realised via a discontinuous scenario. Variation of a model parameter p results in the disappearance of the locally stable node at the curve of discontinuity of the model function (either G_1 or G_2). This mechanism is conceptually similar to that of the single species model (3), the scaling law of the transient lifetime is given by $\tau \propto -\log|p - p_c|$. For both above types of ghost attractors, we can measure the lifetime based

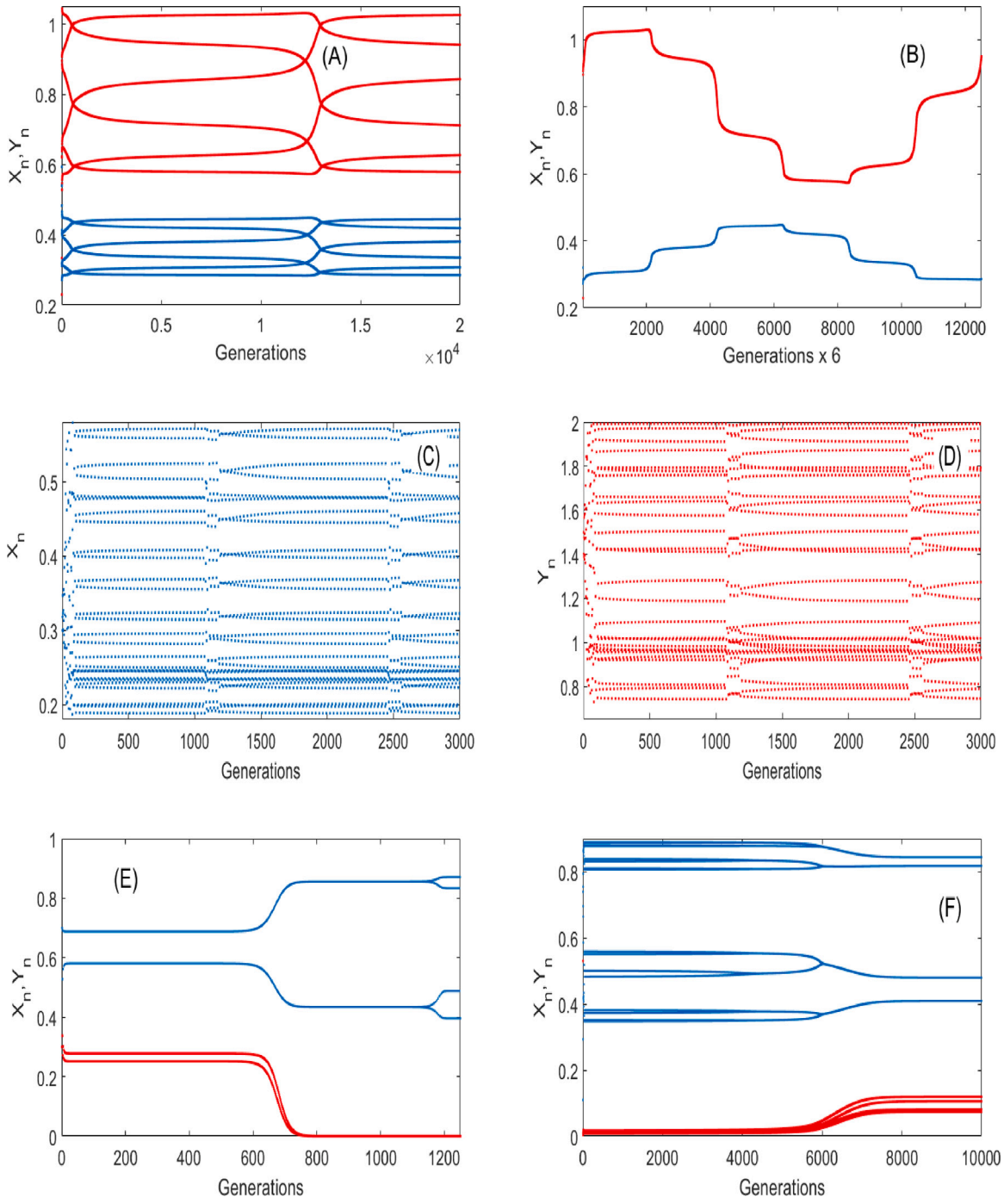

Fig. 5. Main non-chaotic types of long transients in the predator–prey model (8). (A) Transients generated by a ghost attractor via a smooth scenario, $\epsilon = 0.00011$; $\mu = 2.822$; $c = 0.3$; $d = 3.65$; $X_0 = 0.32$; $Y_0 = 0.23$; (B) Variation of prey and predator density for the pattern shown in (A) plotted for every $6k$ generations ($k = 1, 2, \ldots$). (C)-(D) Transients generated by a ghost attractor via a discontinuous scenario, $\epsilon = 0.009195$; $\mu = 3.67$; $c = 0.01$; $d = 3.1196$; $X_0 = 0.3$; $Y_0 = 1.5$. (E) Transient dynamics in the vicinity of a regular saddle point (crawl-by dynamics) resulting in a long coexistence of predator and prey before the predator goes extinct, $\mu = 3.5$, $c = 0.2$; $d = 1.9$, $\epsilon = 0.0044597$, $X_0 = 0.7$, $Y_0 = 0.3$. (F) Transient dynamics in the vicinity of a regular saddle point (crawl-by) which is followed by shorter transients related to an attractive manifold, $\epsilon = 0.0049$; $\mu = 3.6$; $c = 0.2$; $d = 2$; $X_0 = 0.11$; $Y_0 = 0.53$. Red and blue colours, denote, respectively, the density of predator and prey. For explanations of the mechanisms of transients see the text. (For interpretation of the references to colour in this figure legend, the reader is referred to the web version of this article.)

on closeness of the trajectory to the ghost of the fixed point (e.g. the trajectory should not deviate by 5%–10%).

A regular, i.e. non-chaotic saddle point can produce a long transient, if the trajectory passes close to this point. This type of transients is also called the crawl-by dynamics [5]. It is easy to prove that in this case the transient time near the saddle point is scaled as $\tau \propto -\log|p - p_c|$, where p can be considered as an initial condition. Two examples of a transient due to a saddle point are shown in Figs. 5E,F. In both cases, the existence of a saddle point of considered periodicity was verified by constructing a phase portrait and generating a large numbers of trajectories starting from different initial conditions. Fig. 5E provides an example of crawl-by dynamics where the trajectory is initially attracted to a 2-periodic saddle, then it leaves the saddle, which results in extinction of the predator and the dynamics of the prey density is now governed by Eq. (3). In the resultant single-species model, after spending a long time in the vicinity of an unstable node, the prey density

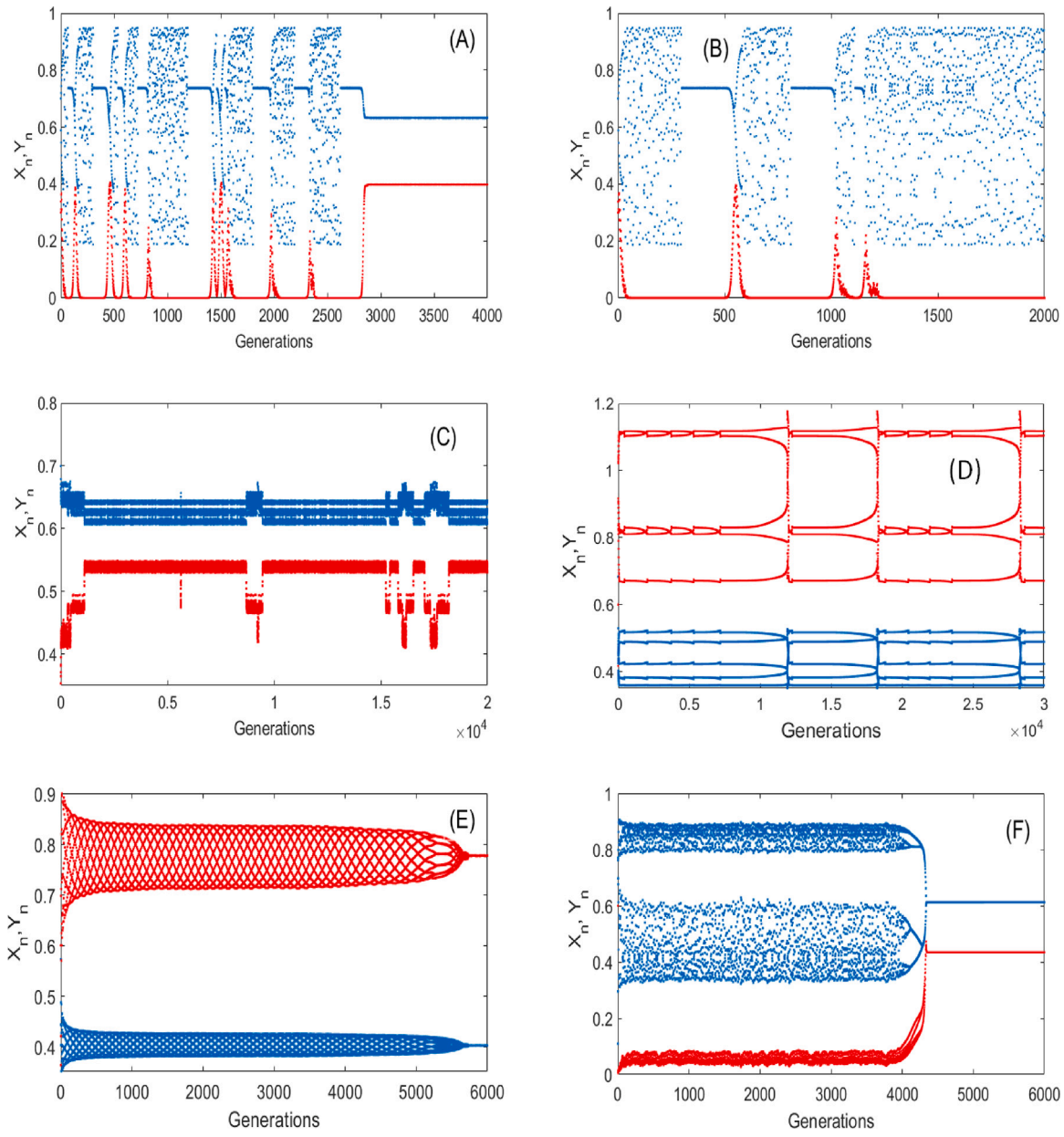

Fig. 6. Long transients involving chaotic behaviour in the predator–prey model (8). (A)-(B) Transient chaotic intermittency characterised by irregular spikes of predator density followed by long periods of low predator density. (A) Coexistence of both species after the transient, $\mu = 3.8$; $\epsilon = 0.002$; $d = 1.9$; $c = 0.2$; $X_0 = 0.7$; $Y_0 = 0.3$. (B) Extinction of the predator at the end of the transient, $d = 1.9$; $c = 0.2$; $\mu = 3.8$; $\epsilon = 0.0015$; $X_0 = 0.7$; $Y_0 = 0.3$. (C) Permanent intermittency with three chaotic phases with oscillations of prey and predator densities within narrow bands, $\mu = 4.1$, $c = 0.2$; $d = 1.9$, $\epsilon = 0.03$, $X_0 = 0.7$, $Y_0 = 0.3$. (D) Chaotic intermittency including transient phases of small and large oscillations of species densities, $d = 3.98$; $c = 0.7$; $\mu = 3.395675$; $\epsilon = 0.0071$; $X_0 = 0.3$; $Y_0 = 0.6$; (E) Transients due to chaotic saddle characterised by oscillations close to quasi-periodic dynamics with a further switch to low amplitude chaotic oscillations, $\mu = 2.97$; $c = 0.56$; $d = 3.88$; $\epsilon = 0.0006$; $X_0 = 0.3$; $Y_0 = 0.6$. (F) Transients due to chaotic saddle characterised by irregular predator–prey oscillations for a long time with a further switching to low amplitude chaotic oscillations, $\mu = 3.77$; $\epsilon = 0.025$; $d = 2$; $c = 0.2$; $X_0 = 0.11$; $Y_0 = 0.6$. Red and blue colours denote, respectively, the density of predator and prey. For explanations see the text. (For interpretation of the references to colour in this figure legend, the reader is referred to the web version of this article.)

approaches its final attractor, a 4-periodic orbit. The scenario shown in Fig. 5F shows a different pattern. Initially, the trajectory is attracted to the vicinity of a 16-periodic saddle point. After leaving the vicinity of the saddle point, the trajectory quickly approaches an attracting manifold which is approximately periodic with the period of $n = 8$. Further, the attracting manifold of the 8-periodic orbit approaches a 4-periodic stable orbit, which is the final attractor of the trajectory. Note that although both the 16-periodic and 8-periodic transient parts look apparently similar by following the dynamics of X_n, Y_n with time, they have different natures from the point of view of the dynamical system. In particular, unlike the 16-periodic transient phase due to a saddle, the 8-periodic transient phase is due to an attracting manifold. Staying on the mentioned manifold cannot be made as long as possible by varying parameters or changing initial conditions. The end of a transient in this case can be determined as deviation of the trajectory from the saddle to be higher than some critical value (e.g. 5% of the population density).

Fig. 6 shows long transients which involve chaotic behaviour. These are due to the presence of chaotic saddles and chaotic dynamics characterised by intermittency. In Figs. 6A,B give examples of patterns of chaotic intermittency which are characterised by phases of a very low predator density. During such phases with $Y_n \ll 1$, the dynamics of prey density are mostly governed by Eq. (3). For the given parameters, the single specie model (3) has a chaotic transient characterised by large amplitude oscillations. Moreover, variation of prey density is such

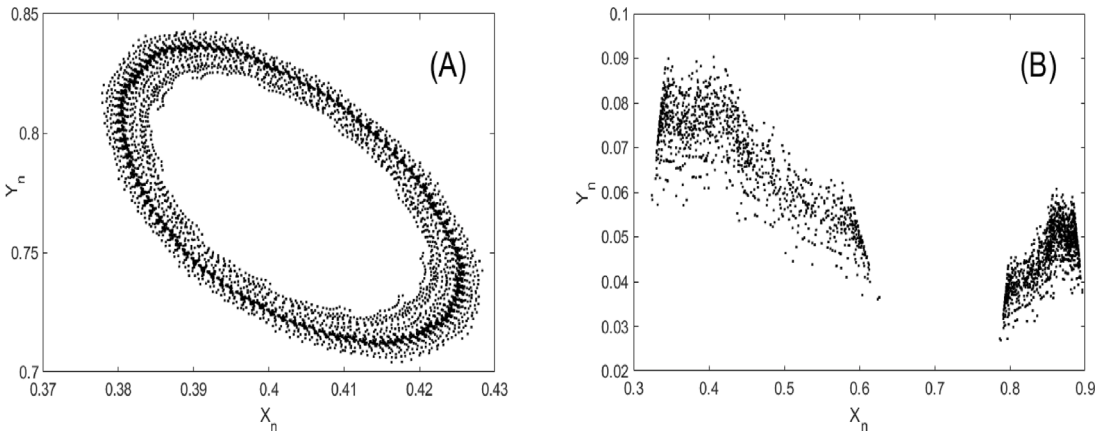

Fig. 7. Examples of chaotic saddles in the predator–prey model (8) producing long transients. Panels (A) and (B) correspond to the transients shown in Figs. 6 E,F. Construction of chaotic saddles was performed using the sprinkler method [42].

that the geometric mean of the per capita growth rate of the predator is smaller than one, thus the predator density declines with time. However, after the chaotic transient (without the predator) ends, the prey density approaches an attractor (chaotic or periodic), which has the property that the geometric mean of the predator per capita growth rate is greater than one. Thus, during this phase the predator density re-starts growing up to values where it begins influencing prey density. However, a spike in the predator density kicks the trajectory to the domain of large chaotic oscillations, where the predator density starts declining again due to the fact that it mean per-capita rate becomes smaller than one. The described intermittent dynamics of spikes and very low density of the predator continues until one of the following outcomes is realised: (i) the trajectory settles at some attractor assuring co-existence of prey and predator (Fig. 6A,) or (ii) the predator density reaches some very low densities where we should considered it to go extinct 6B (this can be formally defined as the end of the transient). Note that similar scenarios are realised in the case prey alone exhibits intermittency dynamics characterised by small and large amplitude oscillations. For both scenarios, we find that the scaling law of the transient lifetime is $\tau \propto \frac{1}{|p-p_c|^\gamma}$, where $\gamma \geq 1$ (see SM5 for the scaling law). As before, the control parameter p is either μ or ϵ.

Other types of transients involving intermittency are shown in Fig. 6C,D. Fig. 6C shows permanent switching between three states with small amplitude chaotic oscillations. Fig. 6D gives an example of intermittency between small and large amplitude chaotic oscillations with almost periodic dynamics. In both cases, intermittent dynamics is asymptotic, i.e. it is the final attractor of the system. In model (8), we find the existence of chaotic intermittency due to smooth and discontinuous scenarios. The end of the transient can be defined the moment when the trajectory leave the trapping region. However, unlike the one-dimensional case, analytical derivation of the critical boundary for the domain for the trapping region for the predator–prey is a complicated task. We find that in a number of cases, some intermittency dynamics can contain non-chaotic transient phases, for example, a saddle point, as shown in Fig. 6D. Fig. 6D shows an example of a hierarchy of transients: the transient with the shortest time scale is due to a saddle point; the trajectory follows other non-chaotic saddles, which is the low amplitude phase of the intermittency regime (in SM5, the scaling is shown for the average length of the ensemble of repeated transient due to non-chaotic saddles).

We find a large variety of transients due to chaotic saddles. Two examples of transients generated by chaotic saddles are shown in Fig. 6E,F (for more examples, see SM4). Chaotic saddles differ in the degree of their chaoticity, for example, this can be measured by their fractal dimension. The chaotic saddle, which generates the transient in Fig. 6E is visually very close to a quasi-periodic curve (see Fig. 7A). For the considered parameters μ, c, d, we find the existence of an invariant close curve – which is a model attractor – in the absence of discontinuity, when $\epsilon = 0$. Adding a small $\epsilon > 0$ results in breaking the invariant curve. The resultant attractor becomes a fractal set, which is still very close to the invariant curve, the corresponding dimension is slightly large than one. A further increase of ϵ transforms the attractor into a set of a finite number of clusters of a small size (each having a fractal structure). The trajectory becomes trapped in each of the clusters and it cannot leave the boundary of the cluster. Finally, an increase of ϵ creates a small escaping channel, thus a long transient emerges. On the contrary, for the transients due to a chaotic saddle (Fig. 6F), the trajectory is not restricted within some narrow regions (clusters) but fills a large portion of the phase plane (the corresponding chaotic saddle is shown in Fig. 7B). The scaling law of the transients due to chaotic saddles can be complicated and be described by several power law dependencies with different exponents (see SM5). The end of chaotic transient can be defined as the time, where the trajectory reaches the vicinity of a new attractor (e.g. being less than 5% of the density).

We investigated the dependence of long transients in (8) on the model parameters. As in the previous section, we are mainly interested in small and intermediate values of parameter ϵ, although transients can be found for larger values of ϵ as well (e.g. up to $\epsilon \approx 1$). Following the same approach as for the single species model, we produced two-dimensional bifurcation diagrams in the plane of parameters ϵ, μ for some fixed values of parameters d and c. We should stress, however, that a clear understanding of the entire structure of the parameter space would require constructing at least several dozens of ϵ, μ portraits for different combinations of d and c. Moreover, as in the single species model, variation of a model parameter by a small value (e.g. by 10^{-5}) can create or suppress a long transient. Therefore, rather than trying to produce an exhaustive multi-dimensional bifurcation portrait of the system, we provide a few insightful examples of parametric diagrams in Figs. 8 and 9. In Fig. 9 we address the important question of the dependence of long transients on the initial condition. Note that some types of transients shown in Figs. 5,6 are not found in the presented bifurcation diagrams since they occur for different values of d and c (we did not find a single two-dimensional parametric diagram which alone contained all possible types of transients). The shown diagrams represents transients due to chaotic saddles and patterns of intermittency, which are the most frequently observed transients in model (8).

From Figs. 8, 9, one can make several important conclusions. Firstly, transients are omnipresent in the predator–prey model. Adding a predator promotes the diversity of transients: this can be seen by comparing the diagrams between the single species and the predator–prey model. Secondly, patterns of transient dynamics observed for small and intermediate values of ϵ differ, in terms of their relative frequency, which is measured as the probability to find a particular type by picking an arbitrary set of model parameters. For small ϵ most of transients are due

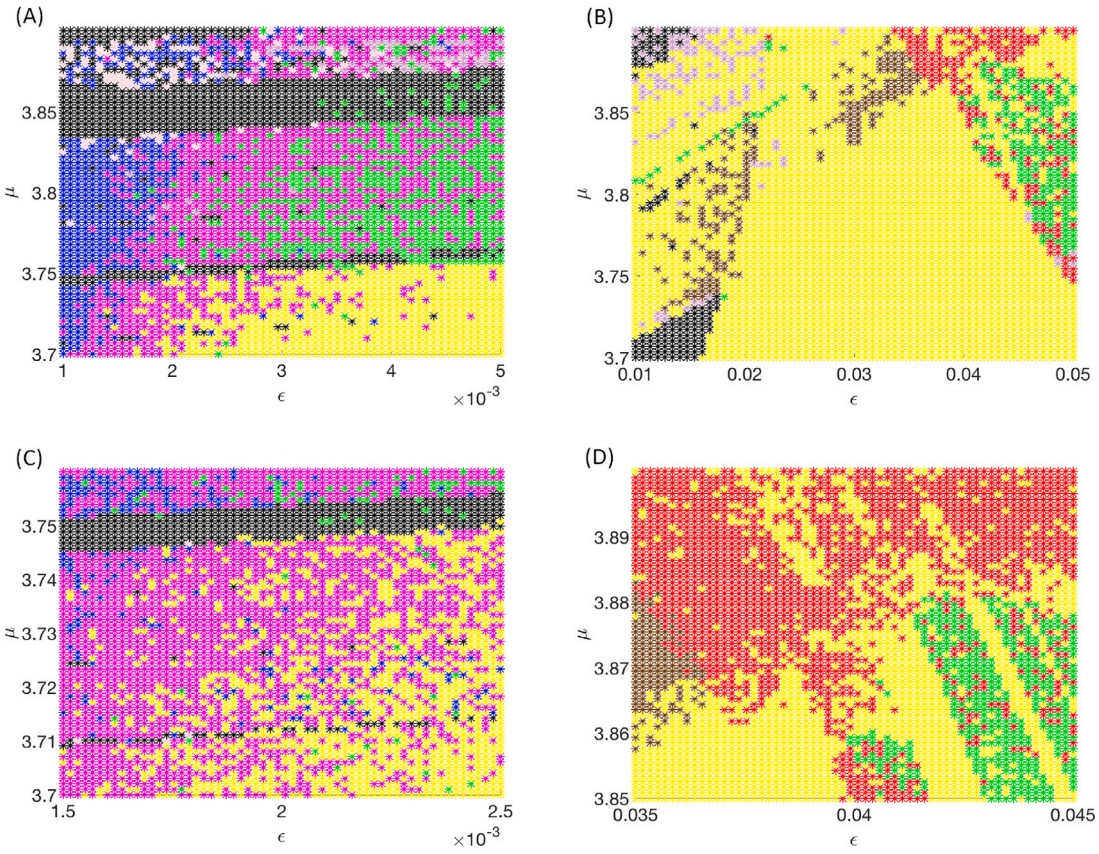

Fig. 8. Dependence of transients on the parameters ϵ and μ for fixed values of $c = 0.2$ and $d = 1.9$ in the predator–prey model (8), with the logistic function for the prey growth. The initial conditions are $X_0 = 0.7$, $Y_0 = 0.3$, the system was simulated within 20,000 generations, first 300 initial iterations are disregarded. A long transient is defined as a pattern which persists within 500 generations. The upper panel shows the diagrams constructed for small and intermediate values of ϵ; the bottom panel provides fine resolutions of the diagrams in the upper panel. The observed long transient patterns include: persistent chaotic intermittency characterised periods of very low predator densities with spikes of high densities (blue); transient intermittency with an eventual extinction of the predator (pastel pink); transient intermittency with further settling at a periodic orbit or a chaotic orbit with chaotic oscillations with small amplitude (magenta); initial quick drop of the predator density to low values with its further recovering: the final system attractor is a periodic orbit or a chaotic orbit with chaotic oscillations with small amplitude (pastel violet); cascade of transients occurring by staying in vicinity of several chaotic saddles (red); transients due to non-recurrent chaotic saddle with a further transition to chaotic oscillations (sepia); quick extinction of predator and transient chaotic intermittency of prey (black). Other colours denote realisations of trajectories without long transients with the final attractors being: a stable periodic orbit or an orbit with chaotic oscillations with a small amplitude approximately equal to ϵ (green); chaotic oscillations (yellow). (For interpretation of the references to colour in this figure legend, the reader is referred to the web version of this article.)

to chaotic intermittency with slow and fast dynamics. In particular, for small values of ϵ, a large proportion of transients with intermittency is characterised by phases with a very low density of predator. An increase in the degree of discontinuity of the map (a larger ϵ) makes a shift towards transients due to chaotic saddles, where the trajectory fill the space in a close to uniform manner. Thirdly, zooming in some parts of the diagrams shows a high sensitivity of transients to parameter variation. The boundary between different transient regimes is close to fractal. From the comparison between Figs. 8 and 9, one can see that a relatively small variation of model parameters d (an increase of 5%) results in a tremendous difference between the parameter diagrams. Similar observation is true for considering other close values of d, c (not shown results). This signifies that the entire parametric space has an extremely complex structure without a clear indication of where transient parameters of particular types should be. Finally, we briefly addressed the dependence of the transients on the initial condition, which is demonstrated in Fig. 9. One can see from the comparison of the right and the left columns of the figure, some types of transients can be only observed starting from particular sets of initial conditions. Moreover, the parametric domain corresponding to long transients can largely alter by modifying initial conditions.

3.3. Influence of noise on long transients

Along with the deterministic version of the model(s) formulated in Section 2, we briefly explore the scenario, where some model parameters are affected by external noise, which is a fairly realistic situation in ecology. Specifically, here we assume that the parameters μ and d exhibit small random fluctuations. Fluctuation of the mentioned parameters at each time step n are described by $\mu_n = \mu_0(1 + \delta_0\xi_n)$ and $d_n = d_0(1 + \delta_0\zeta_n)$, where δ_0 denotes the level of noise ($\delta_0 \ll 1$); ξ_n and ζ_n are random numbers normally distributed with the zero mean and the unit variance; thus, μ_0 and d_0 are the mean values of fluctuating parameters. In this study, we considered the scenario, where ξ_n and ζ_n are described by fractional Brownian motion [43,44]. Fractional Brownian motion is quantitatively characterised by the Hurst exponent H: for negative correlations in fluctuations we have $0 < H < 0.5$, whereas for positive correlations we have $0.5 < H < 1.0$; finally, in the absence of correlations we have $H = 0.5$, which is the classical white (Gaussian) noise. To generate a sequence of random numbers ξ_n and ζ_n based on fractional Brownian motion, we used the computational algorithm from [43].

Our extensive numerical simulations of the single species and the predator–prey models with white noise revealed the following properties. For the existing patterns of transients due to saddles (chaotic

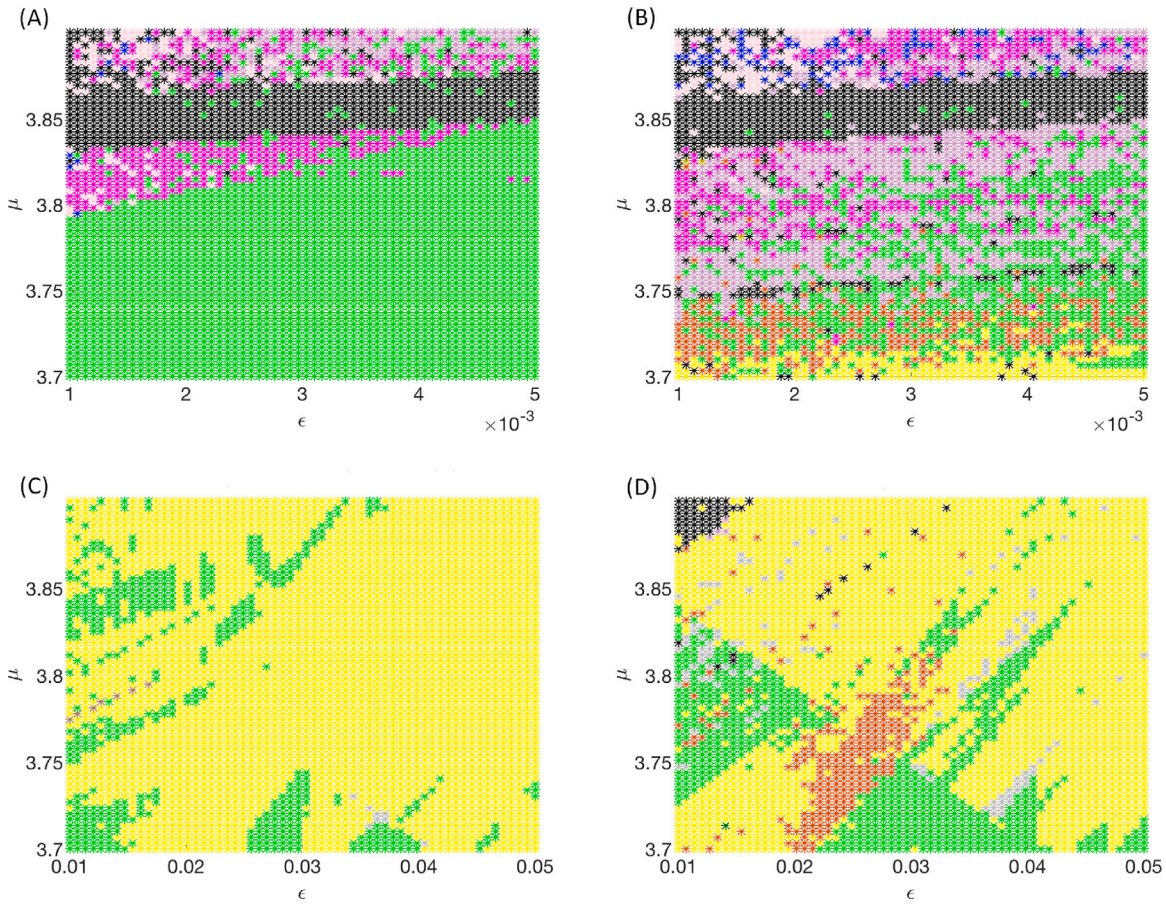

Fig. 9. Dependence of transients on the parameters ϵ and μ for fixed values of $c = 0.2$ and $d = 2.0$ in the predator–prey model (8), with the logistic function for the prey growth. The diagrams in the left column are constructed for the initial conditions $X_0 = 0.7$, $Y_0 = 0.3$, whereas the diagrams in the right column are constructed for $X_0 = 0.11$, $Y_0 = 0.53$. The system was simulated within 20,000 generations, first 300 initial iterations are disregarded. A long transient is defined as a pattern which persists at least within 500 generations before switching to another quasi-stable regime. The upper panel shows the diagrams constructed for small and intermediate values of ϵ; the bottom panel provides fine resolutions of the diagrams in the upper panel. The colours denote the same regimes as in Fig. 8, except the following colours added to denote: transients due to non-recurrent chaotic saddle with large amplitude oscillations with a further settling at a periodic orbit or a chaotic orbit with chaotic oscillations with small amplitude (orange); staying near a non-chaotic saddle with recurrent returns to this saddle (light brown); recurrent chaotic intermittency with phases of slow and fast dynamics (dark green); transients due to chaotic saddle with eventual extinction of predator (olive); quick settling of the trajectory on a quasi-periodic attractor without a long transient (grey). (For interpretation of the references to colour in this figure legend, the reader is referred to the web version of this article.)

or non-chaotic) and ghost attractors in a noise-free system, adding noise generally reduces the length of transients. Note that due to the probabilistic nature of fluctuations, we always obtain a distribution of transient lifetimes: we found that the mean value of this distribution decreases with an increase of the level of noise δ_0. For the predator–prey model, Fig. 10A,B provides an insightful example of transformation of the chaotic transient previously shown in Fig. 6E under the action of a white noise. From Fig. 10B one can conclude that a strong level of noise destroys the original shape of chaotic transient. A similar scenario can be observed by comparing panels (C)-(E) in Fig. 10: the initial chaotic saddle observed until time $T = 2600$ for $\delta_0 = 0$ substantially shrinks in the presence of noise (note that a further increase of noise can produce a different, new pattern of transients, as in Fig. 10F, see the next paragraph). We found reduction of the average transient lifetime in the presence of noise for other types of transients too, both in the single species and the predator–prey model (we do not show the corresponding graphs for the sake of brevity).

On the other hand, allowing for stochasticity in the system can generate new transients, in particular, this concerns regimes of intermittency. An example of noise-induced transients is shown in Fig. 10 D, where noise generates recurrent switch between two levels of species densities: the system remains at a particular state over a long time before switching to the other state. We emphasise that the mean lifetime of noise-induced transients can be made as long as possible by decreasing the level of noise; therefore, our definition of a long transient regime given in Section 2 remains applicable. A further increase of the level of noise results in a fast switch between the states (see Fig. 10 E), therefore no long transients are observed. For a higher level of noise (Fig. 10 E) noise-induced intermittency resumes; however, this pattern is characterised by a switch between the states with a high and very low density of predator. Another example of noise-induced intermittency (in the single-species model) is provided in SM6.

A question may arise here as to how different can be the effect of stochasticity in case noise is not white. Correspondingly, we briefly explored the effect of correlations in the stochastic fluctuation on the occurrence and the length of transient dynamics. We found that for the same level of noise δ_0, the effect of correlated (coloured) noise is highly variable. In some cases, anti-correlated noise ($H < 0.5$) apparently prevents formation of transients, whereas positively correlated noise can create a newlong transient characterised by an abrupt shift to another regime (see Fig. 11 A,B); after the shift the system further remains at the new state. Positive correlations in random variation of model parameters (i.e. $H > 0.5$) generally tend to impede intermittency regimes. The corresponding examples can be seen in Figs. 11 C,D for the predator–prey model and in SM6 for the single species model. On the other hand, Finally, we found that triggering noise-induced transients require a supercritical level of noise: below the threshold, adding noise only results in blurring trajectories around an attractor without any regime shift (see the diagram in SM6).

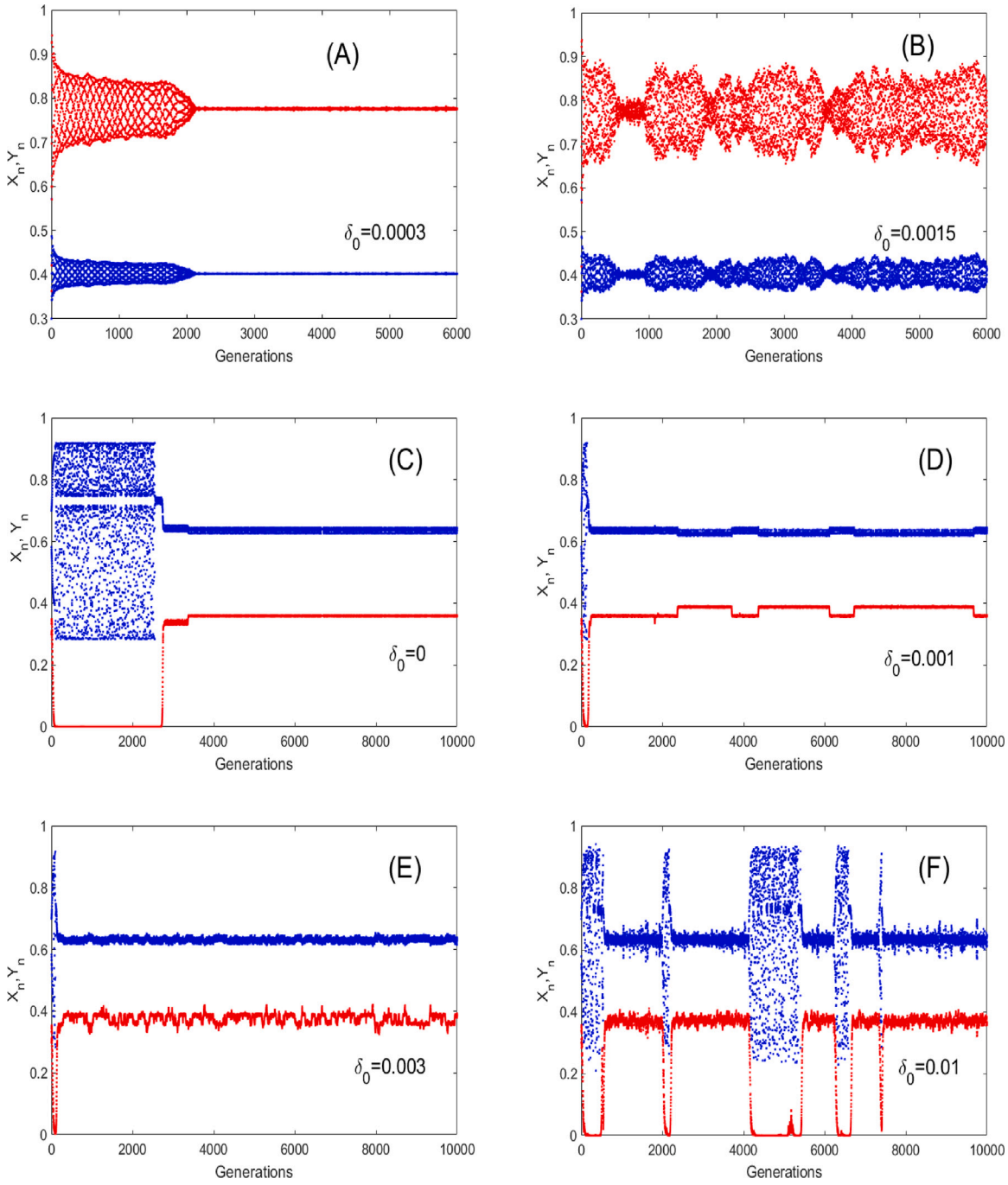

Fig. 10. Influence of the amplitude δ_0 of white noise on long transients in the predator–prey model (8). Variation of the parameters μ and d is described by white (uncorrelated) noise, where the Hurst exponent is $H = 0.5$. (A)-(B) Reduction and eventual suppression of long transients due to a chaotic saddle with an increased δ_0. The transient pattern in the same system without noise is shown in 6E. The other model parameters are as in Fig. 6E. (C)-(F) Gradual alteration of transient patterns for an increased δ_0. The model parameters and the initial conditions are $\mu_0 = 3.7295234$; $\epsilon = 0.015$; $d_0 = 1.9$; $c = 0.2$; $X_0 = 0.7$; $Y_0 = 0.3$. Red and blue colours, denote, respectively, the density of predator and prey. (For interpretation of the references to colour in this figure legend, the reader is referred to the web version of this article.)

To conclude, we stress that the several examples shown in this section with regard to the influence of noise on long transients are by no means exhaustive due to the high complexity of the system. A separate future study should address this problem in more detail.

4. Discussion

Despite a growing recognition of the importance of long transients in ecology, epidemiology as well as neuroscience [1,2,5–8,40], currently theoretical literature is still mostly focused on systems' attractors. The overall goal of this study is to strengthen the message about a key role that transient regimes, especially long transients, can play in population dynamics, and consequently, in ecosystem management and species conservation. We consider two generic time-discrete models of population dynamics: a single-species model and a predator–prey system. The particularity of the considered models is the presence of a discontinuity in the underlying maps. The mentioned discontinuity is introduced to mimic an ecologically realistic scenario, where the species dispersal is density dependent: in particular, it depends on the differences between the population density before and after the

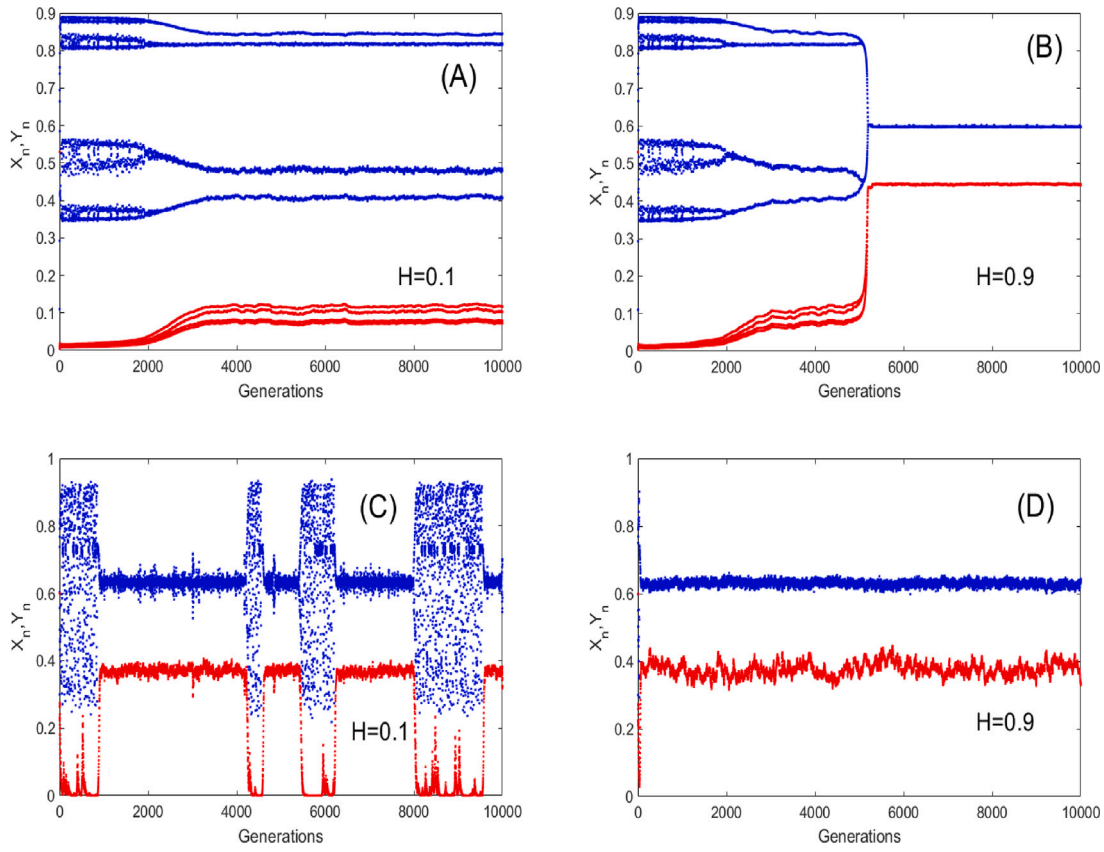

Fig. 11. Influence of negative and positive correlations in the stochastic variation of μ and d on the generation of long transients in the predator–prey model (8). Both μ and d are varied based on the fractional Brownian motion characterised by the Hurst exponent H; for details see the text. (A)-(B) Noise-induced transients are impeded by anti-correlated noise ($H = 0.1$), whereas by positive correlations in parameter variation ($H = 0.9$) can create transients (in both cases the noise level is $\delta_0 = 0.0005$). The model parameters and the initial conditions are $\mu_0 = 3.6$; $\epsilon = 0.00491$; $d_0 = 2$; $c = 0.2$; $X_0 = 0.11$; $Y_0 = 0.53$. (C)-(D) Noise-induced transients via intermittency scenario are promoted by anti-correlated noise ($H = 0.1$), whereas positive correlations ($H = 0.9$) impede generation of transients (in both cases $\delta_0 = 0.0008$). The model parameters and the initial conditions are $\mu_0 = 3.7295234$; $\epsilon = 0.015$; $d_0 = 1.9$; $c = 0.2$; $X_0 = 0.3$; $Y_0 = 0.6$. Red and blue colours, denote, respectively, the density of predator and prey. (For interpretation of the references to colour in this figure legend, the reader is referred to the web version of this article.)

reproduction and growth stages. The use of the considered type of discontinuity is typical in problems of harvesting and control of target species, such as pests, or protected species under the threat of extinction [25–28,45].

From the mathematical point of view, we addressed the following two principle questions: (i) whether the presence of a discontinuity in the map can generate various types of long transients and (ii) whether long transients are frequent in the space of model parameters (by revealing the structure of the parameter space corresponding to transient regimes). We emphasise that transients in piece-wise continuous time-discrete systems are studied much less than in similar systems with smooth maps. This is a yawning gap in our knowledge, as indeed piece-wise continuous maps generally possess a more complicated bifurcation structure than their smooth analogues [29,45,46]. We use the definition of a transient, which is related to regime shifts (see Section 2). Regime shifts due to long transient dynamics can occur for constant model parameters, and this scenario is considered as an alternative to the classical regime shift paradigm using the tipping points philosophy [6, 9].

Both in the single species model (3) and the predator–prey system (8), we find that the discontinuity in the dispersal term promotes long transients according to various mechanisms. Our simulations show that in the absence of dispersal (i.e. $\epsilon = 0$), the transients become rare to find in the parameter space. On the other hand, the presence of discontinuity, even for a very small value of ϵ (e.g. $\epsilon = 10^{-5}$ or smaller), creates new types of transients which are not possible in the system with $\epsilon = 0$. For example, this concerns the possibility of ghost attractors of periodic orbits realised via a discontinuous scenario, which does not require a saddle–node bifurcation (see Figs. 1A, 2A,B, 5C,D). An important difference between a ghost attractor via the continuous and discontinuous scenarios is the different scaling law of transient lifetime: the lifetime of a discontinuous ghost attractor is scaled as a logarithmic law, whereas for a smooth ghost attractor we observe a power law dependence (see Table 1).

A major impact of the discontinuity is the creation of trapping regions with a characteristic size of ϵ such that the trajectory can stay for a long time before escaping such regions. The existence of such trapping regions leads to the emergence of chaotic saddles of various types. In particular, discontinuity-based trapping regions are responsible for intermittency patterns involving slow-fast dynamics (small amplitude chaotic oscillations inside the trap and large-amplitude oscillations outside). Note that recurrent intermittency characterised by irregular switch between different chaotic regimes was found in other piece-wise discrete systems [30], although for a finite size of discontinuity. In the models considered here, however, the size ϵ can be made as small as possible while still allowing patterns of intermittency.

Another important feature of the observed dynamics is that small traps generated by discontinuity can be absorbing: once the orbit lands into such an absorbing trap, it will be held there forever. Such absorbing traps have very narrow attracting channels, which promotes chaotic transients. The trajectory may exhibit long irregular oscillations before it finally finds a narrow escaping channel which would direct it to its final attractor, the absorbing trap. The corresponding transient lifetime is scaled according to the power law as the amplitude of discontinuity tends to zero (see Table 1). The existence of such absorbing traps with a characteristic size (diameter) of approximately ϵ is an important

phenomenon per se with the implications going well beyond the current study focused on transient dynamics. An orbit inside absorbing traps shows chaotic dynamics, which is observed within a wide range of model parameters, whereas in the same system with $\epsilon \equiv 0$, asymptotic chaotic dynamics can be rarely found. The chaoticity inside the absorbing traps was verified via checking the sensitivity of trajectory to the initial condition and by directly estimating the Lyapunov exponents of the map. However, we should say that, although in the precise mathematical sense the oscillations are chaotic, their magnitude is of the order of ϵ, therefore for $\epsilon \ll 1$, an external observer following time series would be tempted to interpret it as a steady state or periodic dynamics affected by a slight noise (even for a purely deterministic system).

Using extensive simulations we reveal that long transients are omnipresent in both single species and the predator–prey model. This can be seen from the constructed parametric diagrams. We find all main types of long transients previously reported in the literature: transients due to non-chaotic saddles; transients due to non-chaotic ghost attractors; transients generated by chaotic saddles; slow-fast dynamics [5]. Moreover, we have discovered hierarchies of transients, i.e. a 'simple' standard long transient can be a part of a complex, compound transient, each part having its own scaling law for the lifetime (Figs. 1 D,F, 6C,D). There can be also a cascade of transients (Figs. 5,6). The structure of parameter space corresponding to long transients is found to be very complex, which makes any prediction of the population dynamics based on a finite time course difficult, if possible at all. The boundary between transient and non-transient regimes is highly irregular, suggesting a possibility of fractal geometry, although a separate study would be needed to define if it is truly fractal or it is close fractal only within some intermediate scales. Note that only very few previous studies explored the dependence of transient lifetime on model parameters [32].

The complexity of the parameter sets corresponding to long transients can be explained by several factors. For example, for chaotic saddles, a very small variation parameters (or initial condition) would result in a large variation of model trajectory, and, as a result, the time spent travelling through the escaping channel will be highly variable. The maximal time of observation can play a role a well. For the constructed diagrams, the observation time was fixed to be $T = 10{,}000$ (or sometimes $T = 20{,}000$), which can affect the classification: some transient regimes with very large lifetimes could be classified as asymptotic. Therefore, the complexity of the transient parameter set is defined by the value of T. A gradual increase of the observation time would result in shrinking of the domain of transients in the parameter space, for $T \to \infty$, transients would be observed within an infinitely narrow region around the bifurcation curves and this would decrease the complexity of the structure of the parameter set. Our definition of a long transient (Section 2) suggests that there should be a bifurcation value such that the transient lifetime becomes infinitely large. However, when approaching the critical value in the parameter space, one can cross several bifurcation curves, where the transient pattern (of a finite time) can disappear and re-emerge several times before becoming infinitely long. Therefore, from the practical point of view, the requirement of having infinitely large observation time can be relaxed. As such, fixing a finite observation time T is another reason for having a complex boundary of transient regimes. Finally, existence of multiple attractors contributes to the complexity of parameter space. Indeed, there can be escaping channels leading to different attractors for a trajectory trapped in some regions. Therefore, a small variation of parameters (or initial condition) can re-direct the trajectory to take another route to escape to a different attractor.

Our theoretical study has several important messages for ecosystem management, species conservation and, potentially, disease control. Firstly, the existence of long transients makes forecast of population dynamics rather complicated, a major issue being our incapability to distinguish between a transient and asymptotic regimes by simply observing the corresponding time series. Both considered models suggest that some transients can persist for hundreds of thousands of generations, which is well beyond all realistic horizons of prediction. On the other hand, a switch of the system from a long transient to a different state can be abrupt and take only a few generations. In other words, a regime shift according to the long transient scenario would occur almost suddenly and without variation of model parameters. Prediction of regime shifts due to the presence of transients would require implementing dynamical modelling, i.e. choosing a certain model, fitting it to data and predicting its dynamics based on model equations [5]. Secondly, even if we are well aware that the regime of the system under consideration is actually a long transient and our model is correct, it is still hard to predict its lifetime. This is because of the high sensitivity of the transient lifetime to a small variation of model parameters and the initial condition (see Figs. 4, 8, 9). For example, the length of a chaotic transient is generally highly variable (see SM3), so one can only estimate the statistical distribution of the lifetime of a transient, rather than predicting its exact value. Thirdly, we find that transients can occur in cascades, i.e. one transient regime can follow another one, i.e. for a constant set of parameters several regime shifts can occur before the system eventually approaches its asymptotic attractor.

From the ecosystem management point of view, one can be interested in maintaining a transient regime as long as possible, if a switch to another regime is undesirable. For example, we are interested in avoiding a population collapse and species extinction. This task is typical for species conservation [6]. Another practical task consists in intentionally 'destructing' an undesirable ecological transient and pushing the system towards some healthy state. This scenario can happen in pest management as well as in ecosystem restoration [6,47]. For both pre-mentioned tasks, direct manipulating with species densities (e.g. via adding or removing a certain amount of organisms), without changing ecosystem parameters, can provide a solution. For example, to artificially maintain a desirable transient one needs to re-send the trajectory to a vicinity of a ghost attractor or a saddle when the system starts leaving some transient state. In the case where the transient regime can persist for a long time, such an adaptive management strategy does not need frequent (e.g. seasonal) application. This will be convenient from the practical point of view of ecosystem management.

We briefly studied effects of noise on long transients in the population dynamics models: the presence of stochasticity (due to internal or environmental factors) is inevitable in any realistic ecosystem. It was previously reported that noise can affect long transients in deterministic systems in a variety of ways [4,5,7,48,49]. We found that random fluctuation of model parameters would reduce the transient lifetime (on average) for transients due to non-chaotic saddles and ghost attractors by pushing the trajectory away from the vicinity of a fixed point (or its ghost). On the other hand, stochasticity can trigger long transients by kicking the system away from its stable equilibrium or trapping regions [7]. Indeed, the trajectory, which would otherwise stay within a small trap of size $\epsilon \ll 1$, can be repeatedly kicked out by an external noise with a small amplitude. This mechanism would be similar to that previously found in excitable systems [50]. Since trajectory absorbing traps are found in both models (3) and (8) within a wide range of parameters, adding noise to the system will make transients even more omnipresent. Our brief investigation into the effects that different types of noise (e.g. positively or negatively correlated) can have on transients reveals a few distinctly different scenarios, where for the same level of noise, having positive and negative correlations can either suppress or trigger transients. We however stress that further investigation will be needed to properly explore the role of positive/negative correlations in parameter fluctuations on long transients.

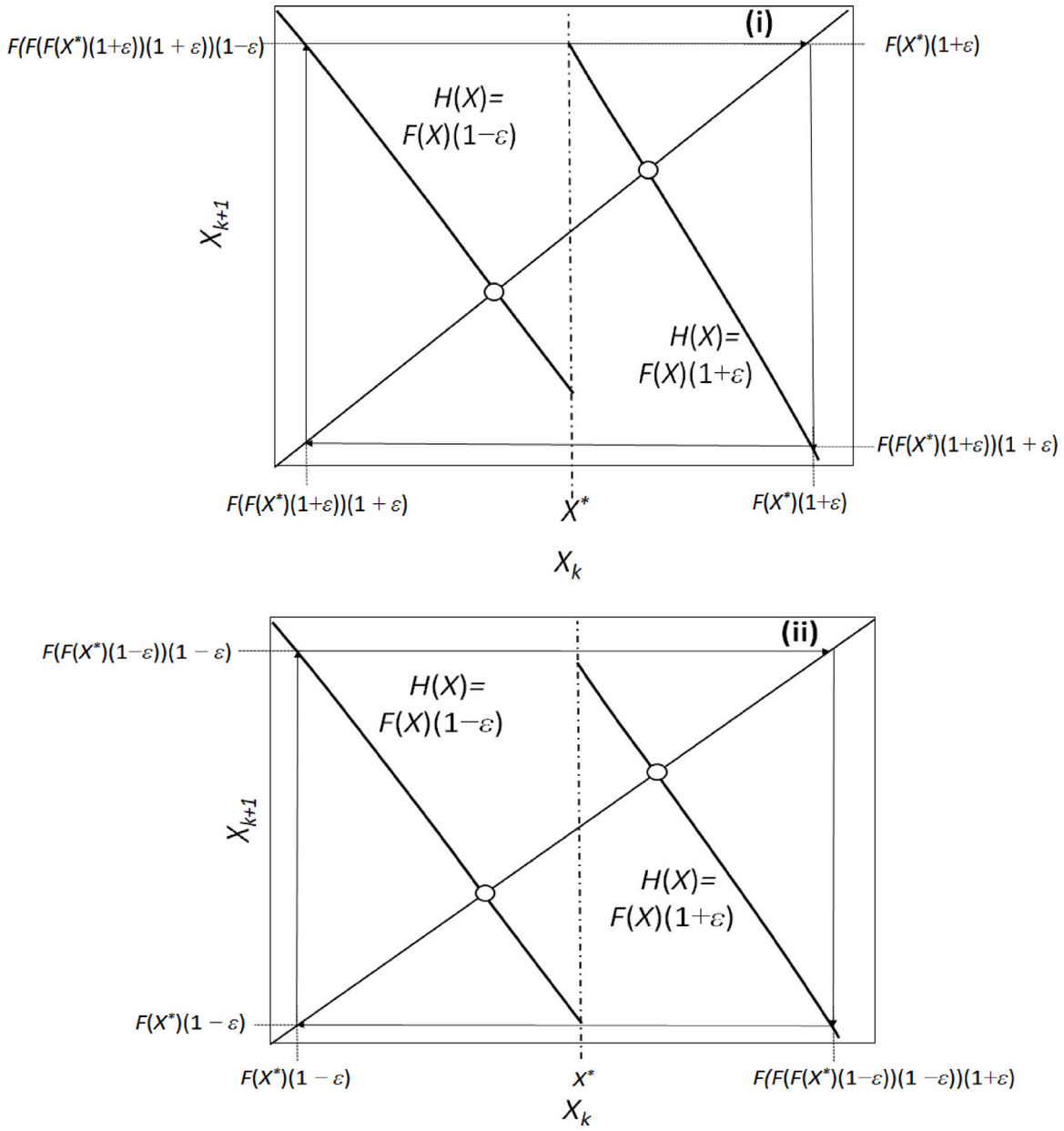

Fig. A. Defining the boundary of the trapping region in the one species model (3) for a generic single-humped function $F(X)$. The trapping region is located around the point of discontinuity of the model X^*. The upper (i) and the bottom (ii) panels show two bifurcation cases considered in the construction of the boundary. For detailed explanations see the text.

5. Conclusions

In this paper, we emphasise the importance of long transients in models in ecology which utilise discrete maps. Here we consider a single species model as well as a predator–prey system. In both models, dispersal of species is assumed to be density dependent and is characterised by discontinuity of the underlying map. In each model, we reveal and classify the main types of transients. They are generated by: non-chaotic saddles, periodic ghost attractor, chaotic repellers or/and saddles, and various mechanisms of intermittency (including chaotic and non-chaotic transient phases). We find that the average transient lifetime is scaled according to either the logarithmic law or the power law (see Table 1). The presence of discontinuity largely promotes the emergence of transients since new transient patterns occur which are possible within a wide range of model parameters. The constructed parametric diagrams show a complex structure of domains corresponding to long transients. By allowing for random fluctuation of parameters, we found that stochasticity can shorten, extend or create new types of transients in models of population dynamics.

CRediT authorship contribution statement

Andrew Yu. Morozov: Conceptualization, Investigation, Methodology, Project administration, Supervision, Writing – original draft, Writing – review & editing. **Dalal Almutairi:** Investigation, Methodology, Writing – original draft, Writing – review & editing. **Sergei V. Petrovskii:** Conceptualization, Methodology, Supervision, Validation, Visualization, Writing – original draft, Writing – review & editing. **Ying-Cheng Lai:** Conceptualization, Investigation, Methodology, Writing – original draft, Writing – review & editing.

Declaration of competing interest

The authors declare that they have no known competing financial interests or personal relationships that could have appeared to influence the work reported in this paper.

Data availability

No data was used for the research described in the article.

Acknowledgements

We are thankful to two anonymous reviewers for their valuable comments. Helpful suggestions from Professor Alan Hastings (University of California at Davis, USA) and Professor Antonio Politi (Aberdeen University, UK) are highly appreciated. SVP was supported by the RUDN University Strategic Academic Leadership Program. YCL was supported by the Office of Naval Research, United States under Grand No. N00014-21-1-2323.

Appendix A

Here, for the single species model (3), we derive the expression for the boundary which separates the domain in the parameter space, for which the trajectory X_t gets eventually trapped near the point of discontinuity X^* and stays in the trapping region forever (the point of discontinuity is defined from the condition $X^* = F(X^*)$).

We consider a generic single-humped function $F(X)$, which is suggested to be decreasing around the point of discontinuity. The structure of the trapping region around is shown in Fig. 2C of the main text. There are two main conditions for the trapping region to exist. One condition is that a trajectory starting at some point $X_0 > X^*$ as close as possible to X^* should return after three consecutive iterations to a point $H^3(X_0) < H(X_0)$, i.e. to the left of the first iteration. The corresponding critical condition, beyond which the trapping region does not exist anymore is analytically determined by $\lim_{X\to X^{*+}} H(X) = \lim_{X\to X^{*+}} H^3(X)$, and graphically it is shown in Fig. A, the upper panel. This is equivalent to the following expression $F(X^*)(1+\epsilon) = F(F(F(X^*)(1+\epsilon))(1+\epsilon))(1-\epsilon)$, or

$$X^*(1+\epsilon) = F(F(X^*(1+\epsilon))(1+\epsilon))(1-\epsilon). \tag{A.1}$$

In a similar way, one can derive the symmetric condition for the boundary of the trapping region starting from a point on close to X^* on the left. The corresponding schematic flowchart is shown in the bottom panel in Fig. A. For the trajectory to stay inside the trapping region, we require that starting from a point X_0 as close as possible to X^* from the left, we will return after three consecutive iterations to a point $H^3(X_0) > H(X_0)$, i.e. to the right of the first iteration. The critical condition for the boundary in the parameter space separating the trapping domain becomes $\lim_{X\to X^{*-}} H(X) = \lim_{X\to X^{*-}} H^3(X)$, which is equivalent to $F(X^*)(1-\epsilon) = F(F(F(X^*)(1-\epsilon))(1-\epsilon))(1+\epsilon)$, or

$$X^*(1-\epsilon) = F(F(X^*(1-\epsilon))(1-\epsilon))(1+\epsilon). \tag{A.2}$$

Based on the above, the trapping region near X^* is defined by the system of inequalities

$$X^*(1+\epsilon) < F(F(X^*(1+\epsilon))(1+\epsilon))(1-\epsilon), \tag{A.3}$$

$$X^*(1-\epsilon) > F(F(X^*(1-\epsilon))(1-\epsilon))(1+\epsilon) \tag{A.4}$$

Therefore, for $\epsilon \ll 1$, for parameters inside the domain (A.3) and close to its boundaries, long transients due to slow-fast intermittency can emerge.

Note that for some functions $F(X)$, only one boundary can be feasible. For example logistic function $F(X) = \mu X(1-X)$, with $X^* = (\mu-1)/\mu$, the curve (A.2) becomes unfeasible for positive $\epsilon \ll 1, \mu$, i.e. the required trapping condition starting from the left of X^* is always satisfied.

Appendix B. Supplementary data

Supplementary material related to this article can be found online at https://doi.org/10.1016/j.chaos.2023.113707.

References

[1] Hastings A. Transients: the key to long-term ecological understanding? Trends Ecol Evol 2004;19(1):39–45.
[2] Hastings A, Abbott KC, Cuddington K, Francis T, Gellner G, Lai Y-C, et al. Transient phenomena in ecology. Science 2018;361(6406):eaat6412.
[3] Wilson RS, Hardisty DJ, Epanchin-Niell RS, Runge MC, Cottingham KL, Urban DL, et al. A typology of time-scale mismatches and behavioral interventions to diagnose and solve conservation problems. Conserv Biol 2016;30(1):42–9.
[4] Valenti D, Fiasconaro A, Spagnolo B. Stochastic resonance and noise delayed extinction in a model of two competing species. Physica A 2004;331(3–4):477–86.
[5] Morozov A, Abbott K, Cuddington K, Francis T, Gellner G, Hastings A, et al. Long transients in ecology: Theory and applications. Phys Life Rev 2020;32:1–40.
[6] Francis TB, Abbott KC, Cuddington K, Gellner G, Hastings A, Lai Y-C, et al. Management implications of long transients in ecological systems. Nat Ecol Evol 2021;5(3):285–94.
[7] Hastings A, Abbott KC, Cuddington K, Francis TB, Lai Y-C, Morozov A, et al. Effects of stochasticity on the length and behaviour of ecological transients. J R Soc Interface 2021;18(180):20210257.
[8] Liu A, Magpantay F. A quantification of long transient dynamics. SIAM J Appl Math 2022;82(2):381–407.
[9] Sadhu S. Analysis of the onset of a regime shift and detecting early warning signs of major population changes in a two-trophic three-species predator-prey model with long-term transients. J Math Biol 2022;85(4):1–33.
[10] Lai Y-C, Tél T. transient chaos: Complex dynamics on finite time scales, vol. 173. Springer Science & Business Media; 2011.
[11] Zincenko A, Petrovskii S, Volpert V, Banerjee M. Turing instability in an economic–demographic dynamical system may lead to pattern formation on a geographical scale. J R Soc Interface 2021;18(177):20210034.
[12] May RM. Biological populations with nonoverlapping generations: stable points, stable cycles, and chaos. Science 1974;186(4164):645–7.
[13] Costantino RF, Desharnais R, Cushing JM, Dennis B. Chaotic dynamics in an insect population. Science 1997;275(5298):389–91.
[14] May RM. Simple mathematical models with very complicated dynamics. In: The theory of chaotic attractors. Springer; 2004, p. 85–93.
[15] Allen LJ. Introduction to mathematical biology. Pearson/Prentice Hall; 2007.
[16] Hadeler K, Gerstmann I. The discrete rosenzweig model. Math Biosci 1990;98(1):49–72.
[17] Hastings A, Hom CL, Ellner S, Turchin P, Godfray HCJ. Chaos in ecology: is mother nature a strange attractor? Annu Rev Ecol Syst 1993;1–33.
[18] Turchin P, Ellner SP. Living on the edge of chaos: population dynamics of fennoscandian voles. Ecology 2000;81(11):3099–116.
[19] Jakobson MV. Absolutely continuous invariant measures for one-parameter families of one-dimensional maps. Comm Math Phys 1981;81(1):39–88.
[20] Ott E. Chaos in dynamical systems. Cambridge University Press; 2002.
[21] Grebogi C, McDonald SW, Ott E, Yorke JA. Exterior dimension of fat fractals. Phys Lett A 1985;110(1):1–4.
[22] Grebogi C, Ott E, Yorke JA. Comment on “Sensitive dependence on parameters in nonlinear dynamics”and on “Fat fractals on the energy surface”. Phys Rev Lett 1986;56(3):266.
[23] Grebogi C, Ott E, Yorke JA. Fractal basin boundaries, long-lived chaotic transients, and unstable-unstable pair bifurcation. Phys Rev Lett 1983;50(13):935.
[24] Grebogi C, Ott E, Yorke JA. Super persistent chaotic transients. Ergodic Theory Dynam Systems 1985;5(3):341–72.
[25] Seno H. A paradox in discrete single species population dynamics with harvesting/thinning. Math Biosci 2008;214(1–2):63–9.
[26] Singh BK, Parham PE, Hu C-K. Structural perturbations to population skeletons: transient dynamics, coexistence of attractors and the rarity of chaos. PLoS One 2011;6(9):e24200.
[27] Franco D, Perán J, Segura J. Effect of harvest timing on the dynamics of the Ricker–Seno model. Math Biosci 2018;306:180–5.
[28] Grey S, Lenhart S, Hilker FM, Franco D. Optimal control of harvest timing in discrete population models. Nat Resour Model 2021;34(3):e12321.
[29] Bernardo M, Budd C, Champneys AR, Kowalczyk P. Piecewise-smooth dynamical systems: theory and applications, vol. 163. Springer Science & Business Media; 2008.
[30] Alfaro G, Capeáns R, Sanjuán MA. Forcing the escape: Partial control of escaping orbits from a transient chaotic region. Nonlinear Dynam 2021;104(2):1603–12.
[31] Kantz H, Grassberger P. Repellers, semi-attractors, and long-lived chaotic transients. Physica D 1985;17(1):75–86.
[32] Morozov AY, Banerjee M, Petrovskii SV. Long-term transients and complex dynamics of a stage-structured population with time delay and the allee effect. J Theoret Biol 2016;396:116–24.

[33] Kaszás B, Feudel U, Tél T. Death and revival of chaos. Phys Rev E 2016;94(6):062221.
[34] Jánosi D, Károlyi G, Tél T. Climate change in mechanical systems: the snapshot view of parallel dynamical evolutions. Nonlinear Dynam 2021;106(4):2781–805.
[35] Zhao M, Xuan Z, Li C. Dynamics of a discrete-time predator-prey system. Adv Difference Equ 2016;2016(1):1–18.
[36] Selvam AGM, Jacintha M, Dhineshbabu R. Bifurcation analysis and chaotic behaviour in discrete-time predator prey system. Int J Comput Eng Res 2019;9(4).
[37] Ludwig D, Jones DD, Holling CS. Qualitative analysis of insect outbreak systems: the spruce budworm and forest. J Anim Ecol 1978;315–32.
[38] Shampine LF, Reichelt MW. The matlab ode suite. SIAM J Sci Comput 1997;18(1):1–22.
[39] Gorban' AN, Cheresiz VM. Slow relaxations of dynamical systems and bifurcations of omega-limit sets. Dokl Akad Nauk 1981;261(5):1050–4.
[40] Rabinovich MI, Varona P. Robust transient dynamics and brain functions. Front Comput Neurosci 2011;5:24.
[41] Medeiros ES, Caldas IL, Baptista MS, Feudel U. Trapping phenomenon attenuates the consequences of tipping points for limit cycles. Sci Rep 2017;7(1):1–11.
[42] Hsu G-H, Ott E, Grebogi C. Strange saddles and the dimensions of their invariant manifolds. Phys Lett A 1988;127(4):199–204.
[43] Feder J. Fractals. Springer Science & Business Media; 2013.
[44] Beran J, Feng Y, Ghosh S, Kulik R. Long-memory processes. Long-Mem Process 2013.
[45] Lois-Prados C, Hilker FM. Bifurcation sequences in a discontinuous piecewise-smooth map combining constant-catch and threshold-based harvesting strategies. SIAM J Appl Dyn Syst 2022;21(1):470–99.
[46] Sushko I, Gardini L, Avrutin V. Nonsmooth one-dimensional maps: Some basic concepts and definitions. J Difference Equ Appl 2016;22(12):1816–70.
[47] Schindler DW, Carpenter SR, Chapra SC, Hecky RE, Orihel DM. Reducing phosphorus to curb lake eutrophication is a success. Environ Sci Technol 2016;50(17):8923–9.
[48] Spagnolo B, Valenti D, Fiasconaro A. Noise in ecosystems: A short review. Math Biosci Eng 2004;1(1):185–211.
[49] Valenti D, Fiasconaro A, Spagnolo B. Pattern formation and spatial correlation induced by the noise in two competing species. Acta Phys Polon B 2004;35:1481–9.
[50] Lindner B, Garcıa-Ojalvo J, Neiman A, Schimansky-Geier L. Effects of noise in excitable systems. Phys Rep 2004;392(6):321–424.